Journal of Applied Phycology
https://doi.org/10.1007/s10811-025-03641-7

RESEARCH

Gelidium corneum and its solid by-product from agar extraction are sources of high-value and sustainable lipids

Joana Batista[1,2,3] · Diana Lopes[1,2] · Bruna B. Neves[1,2] · Ana Rita Pais[1,2] · Marisa Pinho[1,2] · Ana S. P. Moreira[1,2] · Tiago Conde[1,2] · Stefano Bonciarelli[4] · Laura Goracci[5] · João Dias[6] · André Aguiar[6] · Pedro Domingues[2] · Hugo Pereira[3] · Maria Rosário Domingues[1,2] · Tânia Melo[1,2]

Received: 6 June 2025 / Revised: 31 July 2025 / Accepted: 6 August 2025

Abstract

The red alga *Gelidium corneum* is commonly harvested for agar extraction, producing significant biomass residue that remains underutilized. *Gelidium corneum* and its residue represent promising sources of high-value compounds, including lipid ingredients, encompassing omega-3 and omega-6 polyunsaturated fatty acids, with potential applications in foods and cosmetics. Algae lipids are quite diverse and complex, however the lipidome of *G. corneum* and its residue, along with their bioactive potential, remain largely unexplored. This study characterized the lipid signatures of *G. corneum* and its residue after agar extraction using reversed-phase liquid chromatography-tandem mass spectrometry (C18-RP-HPLC-MS/MS) and gas chromatography-mass spectrometry (GC-MS) for esterified fatty acids (FAs) profiling. Despite low lipid content (<1% dry weight), *G. corneum* exhibited a higher glycolipid content, while the residue was richer in phospholipids and triacylglycerols. Nine FAs were identified, with FA 20:4 *n*-6 and FA 20:5 *n*-3 more abundant in *G. corneum*, and FA 18:1 *n*-9 and FA 18:2 *n*-6 in the residue, highlighting their nutritional and functional values. Their lipid profile comprised more than 400 lipid molecular species, following the trend of more glycolipids in *G. corneum* and phospholipids in the residue. Complex lipids with bioactive properties were identified in both matrices, expanding our knowledge of the lipid signature of this seaweed. *Gelidium corneum* lipids showed higher antioxidant scavenging activity and great anti-inflammatory potential by inhibiting cyclooxygenase-2 activity. Although neither matrix inhibited α-amylase, residue lipids effectively inhibited α-glucosidase activity. These findings emphasize *G. corneum* and its residue as sources of high-value lipids for sustainable biotechnological applications, including foods, nutraceuticals and cosmetics.

Keywords Macroalgae · Rhodophyta · By-products · Polar lipids · Neutral lipids · LC-MS · Lipidomics

Introduction

Gelidium corneum, formerly known as *Gelidium sesquipedale*, is a red seaweed mainly found in the Atlantic coasts of France, Spain, Portugal and Morocco (Trigueros et al. 2021a; Mouga and Fernandes 2022). This seaweed, also known as Atlantic Agar, is the most widely harvested agarophyte, being commercially exploited as raw material for producing high-quality agar (Trigueros et al. 2021a). The global demand for agar derived from *Gelidium* increased

✉ Tânia Melo
taniamelo@ua.pt

[1] CESAM - Centre for Environmental and Marine Studies, Department of Chemistry, University of Aveiro, Santiago University Campus, 3810-193 Aveiro, Portugal

[2] Mass Spectrometry Centre, LAQV-REQUIMTE, Department of Chemistry, University of Aveiro, Santiago University Campus, 3810-193 Aveiro, Portugal

[3] GreenCoLab - Associação Oceano Verde, Universidade do Algarve, Campus de Gambelas, 8005-139 Faro, Portugal

[4] Molecular Discovery Ltd., Centennial Park, Borehamwood, Hertfordshire WD6 4PJ, UK

[5] Department of Chemistry, Biology and Biotechnology, University of Perugia, Via Elce di Sotto 8, 06123 Perugia, Italy

[6] Iberagar Sociedade Luso-espanhola de Coloides Marinhos S.A., Estrada Nacional 10 km 18, 2830-411 Coina, Barreiro, Portugal

Published online: 06 November 2025

from 250 to 700 t over the past decade. In 2018, *G. corneum* from Morocco accounted for approximately 80% of the total raw material production for the agar industry, a shift attributed to the decline in wild populations, particularly in Portugal, Spain, Korea and Japan (Santos and Melo 2018). The depletion of this natural resource, coupled with Climate Change and the growing demand for *Gelidium*-based agar, has resulted in global shortages of this seaweed's biomass. These sustainability challenges have led to a significant supply-demand imbalance, driving the wholesale price of agar up by nearly threefold (Santos and Melo 2018).

Agar is a valuable hydrocolloid derived from red seaweeds, known for its significant industrial importance, particularly in food, biotechnology, and cosmetic applications, where its gelling and stabilizing properties are highly prized (Martínez-Sanz et al. 2019; López-Hortas et al. 2021; Trigueros et al. 2021b). Agar extraction typically starts with an alkaline pre-treatment, followed by a hot-water extraction under high pressure at temperatures ranging from 90 to 120 °C (Martínez-Sanz et al. 2020). However, extracting this phycocolloid generates large quantities of residual *Gelidium* biomass (15–40% of the initial dry biomass) (Álvarez-Viñas et al. 2019). While most of this material is typically treated as waste and discarded, a portion is repurposed as fertilizer (Errati et al. 2022) with a very low commercial value (Ferrera-Lorenzo et al. 2014; Álvarez-Viñas et al. 2019). Nevertheless, the residual biomass resultant from agar extraction retains a rich chemical composition, containing valuable putative compounds that can be recovered as ingredients to produce new bio-based materials. Although scarcely studied, this residue may have compounds with health-promoting properties, making them suitable for various industrial applications (Martínez-Sanz et al. 2019; Mateus et al. 2024).

Lipids are among the value-added compounds found in *G. corneum* and its residual biomass (Trigueros et al. 2021a, b; Meinita et al. 2023; Ferreira et al. 2024; Mateus et al. 2024). *Gelidium corneum* is primarily valued for agar extraction. Still, it also contains nutritionally important fatty acids (FAs), particularly the omega-3 ($n-3$) and the omega-6 ($n-6$) polyunsaturated fatty acids (PUFAs), which account for 14 to 43% of total FAs (Cavaco et al. 2021). Among the $n-6$ PUFAs, *G. corneum* contains linoleic acid (FA 18:2 $n-6$), an essential FA that must be obtained through the diet as the human body cannot synthesize it naturally (Spector and Kim 2015), and arachidonic acid (FA 20:4 $n-6$), a precursor of biologically active lipid mediators that play a role in inflammation and, thus, in health and disease (Zhang et al. 2023). Regarding the $n-3$ PUFAs, this seaweed contains eicosapentaenoic acid (FA 20:5 $n-3$; EPA), which has a plethora of biological activities, including anti-inflammatory and cardioprotective properties (Oppedisano et al. 2020). Therefore, this seaweed can be a natural source of healthy and bioactive PUFAs, and other lipids in its composition, for use in food and nutraceutical applications. In fact, *G. corneum* is approved for human consumption by US Food and Drug Administration (Matos et al. 2020) and was recently classified by the European Union as not novel in food (FIP 2025).

Beyond its nutritional applications, this seaweed shows significant potential for the cosmetic industry, offering a rich source of bioactive PUFAs that support skin health and wellness (Ahmad and Ahsan 2020) and prevent skin inflammatory diseases (McCusker and Grant-Kels 2010; Ahmad and Ahsan 2020). This seaweed also supports the use of neutral base lipids, such as palmitic acid (FA 16:0) and oleic acid (FA 18:1 $n-9$), which can be used as emulsifiers, emollient and moisturizing ingredients (Mank and Polonska 2016; Abedi et al. 2020; Atef et al. 2022; Pereira et al. 2025).

However, although the FAs content and profile of *G. corneum* have been examined in some studies (Grina et al. 2020; Matos et al. 2020; Cavaco et al. 2021; Taouam et al. 2024), the FAs composition of its residual biomass after agar extraction, as well as the lipid signature of both *G. corneum* and its residue remain scarcely explored, hindering the full potential and industrial value of this seaweed and the reused of the waste from its industrial processing. Although some studies have investigated *G. corneum* residues after agar extraction as a source of sustainable polysaccharides (Tůma et al. 2020) and for producing protein-rich extracts as added-value ingredients (Mateus et al. 2024), there are no studies focusing on the lipid profiling of *G. corneum* profiling of *G. corneum* residues or their potential applications as a reusable resource.

To the best of our knowledge, only three studies (Matos et al. 2020; Cavaco et al. 2021; Taouam et al. 2024) have characterized the FAs profile of *G. corneum*. Other studies on *G. corneum* residue have reported a low lipid content (Trigueros et al. 2021a, b; Ferreira et al. 2024; Mateus et al. 2024), with only one study providing a detailed FA profile (Ferreira et al. 2024). However, as known from other algae species, FAs (including $n-3$ and $n-6$ PUFAs) are mainly found in complex polar lipids, including phospholipids (PL), glycolipids (GL), and betaine lipids (BT), along with neutral lipids (Lopes et al. 2019a, b, 2020; Rey et al. 2020; Costa et al. 2021; Conde et al. 2025). Polar lipids are known to exhibit a range of biological activities such as anti-inflammatory (Costa et al. 2021; Conde et al. 2025).

Indeed, the detailed lipidome of *G. corneum* and its residual biomass has not yet been characterized. Therefore, this study aims to provide an in-depth characterization of the lipid and FA profiles of *G. corneum* and its residue obtained after agar extraction, using advanced lipidomics approaches based on gas chromatography-mass spectrometry (GC-MS) and liquid chromatography-mass spectrometry (LC-MS), and contribute for the bioprospecting of its lipids by evaluating their antioxidant, anti-inflammatory and anti-diabetic

properties. This will contribute to the exploitation of this macroalga and its residue as an alternative and sustainable source of high-value lipid ingredients for the food, nutraceutical, cosmetic and cosmeceutical industries. By harnessing residual biomass to obtain lipids, in alignment with zero-waste goals, this study can facilitate the utilization of this residue within a circular economy framework and a biorefinery context. This can contribute to reducing the environmental impact and to address sustainability concerns associated with the harvesting *G. corneum* biomass from the wild stocks for agar extraction (Mouga and Fernandes 2022).

Material and methods

Reagents

HPLC-grade dichloromethane, HPLC-grade methanol, perchloric acid ($HClO_4$) 70% and analytical reagent grade ethanol were from Fisher Scientific Ltd. (UK). Milli-Q water was obtained using the Milli-Q Millipore system (Synergy, Millipore Corporation, USA). D-(+)-Glucose, orcinol ($C_7H_8O_2$, 97%), potassium persulfate, 6-hydroxy-2,5,7,8-tetramethylchromane-2-carboxylic acid (Trolox) and methyl nonadecanoate (≥98 %) were from Aldrich (USA). Ascorbic acid was from VWR Chemicals (Leuven, Belgium) and sulfuric acid (H_2SO_4, 95% solution in water) was from Acros Organics (Geel, Belgium), ammonium molybdate ($(NH_4)_6MoO_4.H_2O$) and 2,2'-azino-bis-(3-ethylbenzothiazoline-6-sulfonic acid) diammonium salt (ABTS) were from PanReac (Spain), while 2,2-diphenyl-1-picrylhydrazy radical ($DPPH^{\bullet}$) was from Aldrich (USA). Sodium dihydrogen phosphate dihydrate was from Riedel-de Haën (Germany). Phospholipid standards 1,2-dimyristoyl-*sn*-glycero-3-phosphate (dMPA, PA 14:0/14:0), 1,2-dimyristoyl-*sn*-glycero-3-phosphocholine (dMPC, PC 14:0/14:0), 1,2-dimyristoyl-*sn*-glycero-3-phosphoethanolamine (dMPE, PE 14:0/14:0), 1,2-dimyristoyl-*sn*-glycero-3-phospho-(10-rac-)glycerol (dMPG, PG 14:0/14:0) and 1,2-dipalmitoyl-*sn*-glycero-3-phosphatidylinositol (dPPI, PI 16:0/16:0), 1,2-dimyristoyl-*sn*-glycero-3-phospho-L-serine (dMPS, PS 14:0/14:0), 10,30-bis[1–dimyristoyl-*sn*-glycero-3-phospho]-glycerol (tMCL, $(CL14:0)_4$), 1-nonadecanoyl-2-hydroxy-*sn*-glycero-3-phosphocholine (LPC 19:0) and N-heptadecanoyl-D-*erythro*-sphingosylphosphorylcholine (SM 18:1;2O/17:0), and N-heptadecanoyl-D-*erythro*-sphingosine (Cer 18:1;2O/17:0) were from Avanti Polar Lipids, Inc. (USA).

Seaweed material

Gelidium corneum and its residue, obtained after agar extraction, were kindly provided by Iberagar-Sociedade Luso-Espanhola de Colóides Marinhos S.A. (Coina, Portugal). The *G. corneum* samples were harvested in the west coast of Portugal, in August (Summer). The harvesting process involved manual cutting by a diving team, in transects of 100 m, at a depth of approximately 10 m, sampling as many different populations as possible. All samples were then subject to a sun drying process, transported and stored in dry conditions. The samples were received dried, milled, and stored in hermetic plastic bags in the dark at room temperature until use. For agar extraction, the *Gelidium* biomass was washed to remove sand, salts, shells and other foreign matters. Afterwards, it was subjected to an alkaline pre-treatment, with sodium hydroxide, for approximately 1 h at 90 ºC, before being placed in tanks for extraction with hot water. After the pre-treatment, a hot-water extraction was performed, at high pressure and around 110 ºC. The hot extract was subjected to coarse filtration to remove the seaweed residue, filter aid is added, and the extract is pumped through a filter press equipped with a fine filter cloth. After cooling, the gel formed from the extract was subjected to a freeze-thaw process to remove the water.

Lipid extraction procedure

Lipids from *G. corneum* and its residue ($n = 5$ replicates) were extracted following the Bligh and Dyer method with modifications (Lopes et al. 2020). 250 mg of each biomass was mixed with 1.25 mL of dichloromethane and 2.5 mL of methanol in a glass PYREX tube and homogenized by vortexing for 2 min. The samples were incubated on ice for 2.5 h on an orbital shaker, at 150 rpm and then centrifuged for 10 min at 2000 rpm. The supernatant was collected in a new glass PYREX tube and the pellet was re-extracted three more times with 1.25 mL of dichloromethane and 2.5 mL of methanol. The combined supernatants were dried under a nitrogen stream, re-dissolved in 2 mL of dichloromethane and 2 mL of methanol and vortexed. Then, 1.88 mL of Milli-Q water was added followed by 2 min of vortexing and centrifugation for 10 min at 2000 rpm. The organic phase was collected to a new glass PYREX tube, and the aqueous phase was re-extracted twice with 2 mL of dichloromethane. The combined organic phases were dried under a nitrogen stream. Lipids were transferred to pre-weighted amber vials, dried again under a nitrogen stream, weighed, and stored at −20 °C for further analysis. The lipid content was estimated by gravimetry and expressed as percentage of dry weight (% DW), following the equation:

$$Lipid\ content\left(\%\ DW, \frac{w}{w}\right) = \frac{Weight\ of\ lipid\ extract\ (mg)}{Weight\ of\ biomass\ (mg)} \times 100$$

Phospholipids quantification

Phospholipids were quantified by measuring the phosphorus amount using a modified version of the molybdovanadate method as described previously (Couto et al. 2021). Dried aliquots of 25 µg of total lipid extracts from *G. corneum* and its residue, and standards of 0 to 2 µg of phosphorus (100 µg mL^{-1} in Milli-Q water, $NaH_2PO_4.2H_2O$) were resuspended in 125 µL of 70% perchloric acid. Only the samples were incubated in a heating block at 180 °C for 1 h and cooled to room temperature. Then, 825 µL of Milli-Q water, 125 µL of 2.5% ammonium molybdate solution (2.5 g (100 mL)$^{-1}$ Milli-Q water), and 125 µL of 0.1% ascorbic acid solution (0.1 g (100 mL)$^{-1}$ Milli-Q water) were added to the samples and standards, with vortex mixing after each addition. Samples and standards were incubated for 10 min at 100 °C in a water bath. After cooling, a volume of 200 µL of samples and standards was placed on a microplate and the absorbance was measured at 797 nm in a microplate UV-vis spectrophotometer (Multiskan GO, Thermo Scientific, USA). The PL content was estimated by multiplying the amount of phosphorus by 25 (Weinman et al. 1950).

Glycolipids quantification

Glycolipids (GL) were quantified by measuring the total carbohydrates using the orcinol method as described previously (Couto et al. 2021). Dried aliquots of 25 µg of total lipid extracts from *G. corneum* and its residue, and standards of 0 to 50 µg of glucose (2.0 mg mL^{-1} in methanol) were resuspended in 1 mL of orcinol solution (0.2% in 70% H_2SO_4) and incubated at 80 °C for 20 min. The tubes were cooled to room temperature and 200 µL of samples and standards were placed in a microplate. The absorbance was measured at 505 nm in a microplate UV-vis spectrophotometer (Multiskan GO). The GL content was estimated by the conversion factor 100/35 (Bell et al. 1987).

Triacylglycerols quantification

Triacylglycerols (TG) were quantified using a commercial kit (Liquick Cor-TG 30 (PZ CORMANY S.A., Poland)), according to the manufacturer's instructions. Vesicles of dried lipids from *G. corneum* and its residue at 4 mg mL^{-1} were prepared in 5 mM ammonium bicarbonate buffer (pH 7.4), as previously described (Conde et al. 2023). Results were expressed in percentage (%).

Pigments quantification

Total chlorophylls and carotenoids present in *G. corneum* and its residue (0.2 µg $µL^{-1}$ of total lipid extracts in methanol) were estimated by measuring the absorbance at 678 nm for chlorophyll and 450 nm for carotenoids using standards of 0, 5, 15, 25, 30 and 40 µg mL^{-1} of each pigment (chlorophyll *a* and fucoxanthin, respectively). Results were expressed as the sum of total chlorophylls and carotenoids (Li et al. 2018; Wang et al. 2018).

Phenolics quantification

Total phenolics were quantified using the Folin-Ciocalteu method as described previously (Libbey and Walradt 1968). Standards of 0 to 0.2 mg mL^{-1} were prepared using a gallic acid solution (0.5 mg mL^{-1} in ethanol). In a microplate, a volume of 15 µL of *G. corneum* and its residue (120 µg total lipid extracts in 36 µL ethanol) or standards were added to the wells, followed by 75 µL of the Folin-Ciocalteu reagent (5-fold-diluted). The plate was incubated for 5 min at room temperature and in the dark. Then, 150 µL of aqueous sodium carbonate solution (7% w/v in Milli-Q water) were added, and the microplate was incubated for 1 h at 30 °C. The absorbance was measured at 750 nm. The results were expressed as gallic acid equivalents (mg) per 100 mg of dried sample.

Analysis of fatty acids by chromatography-mass spectrometry (GC-MS)

Gas chromatography-mass spectrometry (GC-MS) was used to determine the fatty acids profile of *G. corneum* and its residue. Dried aliquots of 50 µg of lipid extracts were dissolved in 1 mL of *n*-hexane containing the internal standard methyl nonadecanoate (FA 19:0; 1.0 µg mL^{-1}). Esterified fatty acids were converted to fatty acid methyl esters (FAMEs) using a methanolic solution of potassium hydroxide (KOH/methanol, 2.0 M) for the alkaline transesterification, as previously described (Lopes et al. 2020). After 2 min of vigorous vortexing, 2 mL of saturated NaCl solution (10 g L^{-1}) was added, and samples were centrifuged at 2000 rpm for 5 min. A volume of 600 µL of the organic phase was collected and dried using a nitrogen stream. The resulting FAMEs were dissolved in 100 µL of *n*-hexane, and a volume of 2 µL was injected on the GC-MS with an autosampler G 4513 A. The GC (Agilent Technologies 8860 GC System, USA) was equipped with a DB-FFAP column (30 m long, 0.32 mm internal diameter, and 0.25 µm film thickness; J&W Scientific, USA). The GC oven temperature was programmed as follows: 58 °C for 2 min, 25 °C min^{-1} to 160 °C, 2 °C min^{-1} to 210 °C, and 30 °C min^{-1} to 225 °C (held for 20 min). The GC equipment was connected to an Agilent 5977B Mass Selective Detector operating with electron impact ionization at 70 eV, scanning range of *m/z* 50–550, and 1 s cycle in a full scan mode. The following conditions were used: inlet temperature at 220 °C, detector temperature at 230 °C, helium as carrier gas (constant flow at 1.4 mL min^{-1}).

The data acquisition software used was GC-MS 5977B/Enhanced MassHunter. Data was analyzed using the software Agilent MassHunter Qualitative Analysis 10.0. FAs were identified by MS spectrum comparison with the chemical database NIST library and "The Lipid Web" (2023) and by considering retention times and MS spectra of FA standards (Supelco 37 Component FAME Mix; Sigma-Aldrich, USA). Quantification was performed by normalization with the internal standard (FA 19:0) (Monteiro et al. 2025). The FA profile was also expressed as a relative percentage considering the total FAs (μg mg^{-1} lipid extract).

Atherogenicity (AI) and thrombogenicity (TI) indices as well as the hypocholesterolemic/hypercholesterolemic (h/H) ratio were calculated using the following equations:

$$AI = \frac{[C12:0 + 4 \times C14:0 + C16:0]}{[\sum n-3\ PUFA + \Sigma n-6\ PUFA + \Sigma MUFA]}$$

$$TI = \frac{[C14:0 + C16:0 + C18:0]}{[(0.5 \times \sum MUFA) + (0.5 \times \sum (n-6)) + 3 \times \sum (n-3)) + (\sum \frac{(n-3)}{(n-6)})]}$$

$$h/H = \frac{[cis - C18:1 + \sum PUFA]}{[C14:0 + C16:0]}$$

Lipidomics analysis

C18 Reversed-phase liquid chromatography-electrospray ionization-mass spectrometry (C18 RP-LC-ESI-MS)

The lipid profile of *G. corneum* and its residue was analyzed by C18 RP-LC-ESI-MS on an Ultimate 3000 Dionex ultra high-performance liquid chromatography (UHPLC) system (Thermo Fisher Scientific, Germany) with an autosampler coupled to the Q-Exactive hybrid quadrupole Orbitrap mass spectrometer (Thermo Fisher). Briefly, 5 μL of a mixture containing 25 μL of *G. corneum* samples in dichloromethane (2 μg μL^{-1} of total lipid extracts), 67 μL of solvent mixture of 50% isopropanol and 50% methanol, and 8 μL of phospholipid standards mixture (dMPC – 0.04 μg, SM (18:1;2O/17:0) - 0.04 μg, dMPE - 0.04 μg, LPC 19:0 - 0.04 μg, dPPI - 0.08 μg, $CL(14:0)_4$ - 0.16 μg, dMPG - 0.024 μg, Cer (18:1;2O/17:0) - 0.08 μg, dMPS - 0.08 μg, dMPA - 0.16 μg), was loaded in the column Ascentis Express C18 column (Sigma-Aldrich, 2.1 x 150 mm, 2.7 μm) at 50ºC and at a flow-rate of 260 μL min^{-1}. A total of five replicates of *G. corneum* and its residue were analysed. The following gradient was applied for the chromatographic separation: 32% B at 0 min, 45% B at 1.5 min, 52% B at 4 min, 58% B at 5 min, 66% B at 8 min, 70% B at 11 min, 85% B at 14 min, 97% B at 18 min, 97% B at 25 min, 32% B at 25.01 min and 32% B at 33 min. Mobile phase A consisted of 40% water and 60% acetonitrile while mobile phase B was composed of 90% isopropanol and 10% acetonitrile, both containing 10 mM ammonium formate and 0.1% formic acid.

The mass spectrometer operated using positive/negative switching toggles between positive (ESI 3.0 kV) and negative (ESI 2.7 kV) ion modes, as previously described (Neves et al. 2025). The capillary temperature was 320 °C, and the sheath gas flow was 35 (arbitrary units). Data were acquired in full scan mode with a high resolution of 70,000 at *m/z* 200, an automatic gain control (AGC) target of 3×10^6, an *m/z* range of 200–1600, 2 microscans, and a maximum inject time (IT) of 100 ms. The tandem mass spectra (MS/MS) were obtained with a resolution of 17,500, an AGC target of 1×10^5, 1 microscan, and a maximum IT of 100 ms. Cycles consisted of one full-scan mass spectrum and ten data-dependent MS/MS scans, continuously repeated throughout the experiments with a dynamic exclusion of 30 s and an intensity threshold of 8×10^4, and the normalized collision energy (CE) ranged between 20, 24, and 28 eV in the negative mode and 25 and 30 eV in the positive mode. Data acquisition was performed using the Xcalibur data system (V3.3, Thermo Fisher Scientific).

Data analysis

Lipid species were identified based on mass accuracy (C18-RP-HPLC-MS data) and typical fragmentation pathways of the respective lipid classes (C18-RP-HPLC-MS/MS data). This analysis allowed the detection of lipid species belonging to phosphatidylcholine (PC), lyso phosphatidylcholine (LPC), phosphatidylethanolamine (PE), phosphatidylglycerol (PG), phosphatidylinositol (PI), phosphatidic acid (PA), monogalactosyldiacylglycerol (MGDG), digalactosyldiacylglycerol (DGDG), acyl monogalactosyldiacylglycerol (acMGDG), acyl digalactosyldiacylglycerol (acDGDG), glucuronosyldiacylglycerol (GlcADG), acyl glucuronosyldiacylglycerol (acGlcADG), ceramide (Cer), hexosylceramide (HexCer), ceramide phosphoinositol (PI-Cer), ceramide phosphoethanolamine (PE-Cer), diacylglyceryl-*N*,*N*,*N*-trimethyl homoserine (DGTS), monoacylglyceryl-*N*,*N*,*N*-trimethyl homoserine (MGTS), hemibismonoacylglycerophosphate (HBMP), bismonoacylglycerophosphate (BMP), cardiolipin (CL), *N*-acyl glycine (NAGly), *N*-acyl glycine serine (NAGlySer), *N*-acyl ornithine (NAOrn), sulfonolipids (SL), sterol lipids (ST), diacylglycerol (DG), and triacylglycerol (TG) classes. The *sn*-position of the fatty acyl chains was attributed according to the LIPID MAPS classification (*sn*−1/*sn*−2 when the position of the

FA is identified; *sn-_sn-* when the position of the FA is not assigned). Raw data import, peak detection, feature detection and identification, and peak area integration were then performed using Lipostar software (Molecular Discovery Ltd., version 2.1.5 × 64) (Goracci et al. 2017). Raw files were imported and an automatic MS signal threshold and a MS/MS signal threshold of 100 was used both for positive and negative ion modes. Feature detection was carried out using the following settings: *m/z* tolerance ±0.02 Da; Chromatogram Filtering Threshold of 0.97; MS/MS filtering threshold of 0.97; Signal Filtering Threshold of 10000. Lipid assignment and identification were performed in both positive and negative ion modes against a database generated in the Lipostar BDManager by importing the LIPID MAPS structure database (version February 2024) and further fragmenting it with Lipostar's fragmentation rules. The raw files were directly imported and aligned according to the settings specified in (Goracci et al. 2017). Automatic peak picking was performed with SDA smoothing level set to high and a minimum S/N ratio of 3. Lipid identification was performed considering only features with MS/MS spectra and according to the following parameters: 5 ppm precursor ion mass tolerance and 20 ppm product ion mass tolerance. Automated approval was executed to retain structures rated between 2 to 4 stars in terms of confidence. The nomenclature and shorthand notation follows the recent LIPID MAPS consensus on classification of MS-derived lipid structures (Liebisch et al. 2020). Lipid annotation and validation for lipid species from DGTS, MGTS, DGDG, MGDG, SQDG, GlcADG, acDGDG, acMGDG, acGlcADG, HBMP, ST, and SL in Lipostar software was based on the MS/MS data analysis since Lipostar v.2.1.5 lacks fragmentation rules for these lipid classes. The validated peaks were within the typical retention time (RT) of the respective lipid class and the exact mass with an error of 5 ppm. For relative quantification, the integrated peak area values of the extracted ion chromatograms (XIC) of each lipid species were exported in the comma-separated values (.csv) format. Data normalization was performed by dividing the XIC peak areas by the XIC peak area of the selected internal standard for the class or by the sum of total peak areas (Tables S1 to S9). For PC, BMP, MGDG, DGDG, SL, DGTS, NAGlySer, NAOrn, and DG the internal standard used was dMPC (PC 28:0). Cer, HexCer, acMGDG, acDGDG, ST and TG were normalized by Cer 35:1;O2 (Cer 18:1;2O/17:0). dMPE (PE 28:0) was used for PE, PE-Cer, SQDG, GlcADG and acGlcADG. For PI and PI-Cer was used dPPI (PI 32:0). For PG, PA, and CL were used dMPG (PG 28:0), dMPA (PA 28:0), and CL 56:0, respectively. The relative abundance (%) of each lipid species within each class was calculated as described in (Pais et al. 2024; Neves et al. 2025).

Screening of biological activities

Antioxidant activity

The antioxidant scavenging activity against the $DPPH^{\bullet}$ and $ABTS^{\bullet+}$ was evaluated as previously described (Melo et al. 2018). Briefly, 150 µL of $DPPH^{\bullet}$ or $ABTS^{\bullet+}$ diluted solution (absorbance of 0.9 at 517 nm or 734 nm, respectively) were mixed with 150 µL of *G. corneum* lipid extracts (final concentration of 50, 100, 250 µg mL^{-1} in ethanol) or 150 µL of Trolox standards (final concentration of 5, 12.5, 25, 37.5 µmol L^{-1} in ethanol). Controls of each sample were also prepared by replacing $DPPH^{\bullet}$ or $ABTS^{\bullet+}$ diluted solution by ethanol. Radical stability (absorbance decrease <10%) was evaluated by mixing 150 µL of $DPPH^{\bullet}$ or $ABTS^{\bullet+}$ diluted solution with 150 µL ethanol. The mixture was incubated for 120 min and the absorbance was measured at 517 nm or 734 nm for $DPPH^{\bullet}$ and $ABTS^{\bullet+}$, respectively each 5 min (Multiskan GO, Thermo Scientific, USA). The analyzes were carried out in triplicate. The antioxidant activity, expressed as percentage of scavenging of the $DPPH^{\bullet}$ or $ABTS^{\bullet+}$ was calculated using the equation:

$$\%\ \text{Scavenging} = \frac{\text{Abs radical} - \text{Abs}_{(\text{samples}-\text{control})}}{\text{Abs radical}} \times 100$$

The concentration of lipid extracts able to scavenge 10 % of $DPPH^{\bullet}$ (SC_{10}) and 30 % of $ABTS^{\bullet+}$ (SC_{30}) was calculated through the linear regression, using the concentration of samples and the percentage of the inhibition curve. The activity was also expressed as Trolox Equivalents (TE, µmol Trolox g^{-1} of sample), using the equation:

$$\text{TE} = \frac{SC_{10}/SC_{30}\ \text{Trolox}\ (\mu\text{mol}\ L^{-1})}{SC_{10}/SC_{30}\ \text{of extracts}\ (\mu g\ mL^{-1})} \times 1000$$

Anti-inflammatory activity

The anti-inflammatory activity was evaluated *in chemico* using the commercial cyclooxygenase-2 (COX-2) inhibitory screening assay (Cayman test kit-701080; Cayman Chemical Company, USA), according to the manufacturer's instructions (Anon 2025b). Lipid extracts of *G. corneum* and its residue were analyzed in duplicate, at concentrations of 50, 100, 250 µg mL^{-1}, prepared in a final volume of 10 µL of DMSO. The inhibition of COX-2 activity was expressed in percentage (%).

Antidiabetic activity

Inhibition of α-amylase activity The ability of lipid extracts from *G. corneum* and its residue to inhibit α-amylase

was evaluated as previously described with modifications (Timalsina et al. 2021). Samples were prepared at three different concentrations (final concentration of 75, 100, 250 µg mL^{-1} in DMSO) followed by vortexing for 5 min. In a 96 plate well, 10 µL of DMSO (negative control), 10 µL of acarbose (20 mg/mL; positive control) or 10 µL of samples were mixed with 80 µL of α-amylase (1.5 U mL^{-1} in 0.1 M phosphate buffer (pH 6.9)) and 10 µL buffer (final volume of 100 µL). The % of DMSO used (5 %) did not cause interference in the assay. The plate was incubated at 37 °C for 15 min (Multiskan GO, Thermo Scientific) followed by the addition of 100 µL of 2-chloro-4-nitrophenyl-α-D-maltotrioside (375 µM in 0.1 M phosphate buffer (pH 6.9)). The plate was incubated at 37 °C for 30 min and the absorbance was read at 405 nm. The inhibition of α-amylase activity was expressed in percentage (%) using the following equation:

$$\% \text{ Inhibition} = \frac{\text{Abs}_{\text{DMSOnegative control}} - \text{Abs}_{\text{sample}}}{\text{Abs}_{\text{DMSOnegative control}}} \times 100$$

Inhibition of α-glucosidase activity The ability of lipid extracts from *G. corneum* and its residue to inhibit α-glucosidase activity was evaluated as previously described (Pais et al. 2024; Neves et al. 2025). Samples were prepared in 0.1 M potassium phosphate buffer (pH 6.9) at three different concentrations (final concentration of 75, 100, 250 µg mL^{-1}) by vortexing for 5 min and sonicating for 15 min to form vesicles (Conde et al. 2023). In a 96 plate well, 50 µL buffer solution (negative control), 50 µL acarbose (10 mg mL^{-1}; positive control), or 50 µL of each sample were mixed with 100 µL α-glucosidase (1.0 U mL^{-1} in 0.1 M phosphate buffer (pH 6.9)). The plate was incubated at 25 °C for 10 min (Multiskan GO, Thermo Scientific, USA) followed by the addition of 50 µL of substrate (5 mM ρ-nitrophenyl-α-D-glucopyranoside in 0.1 M phosphate buffer (pH 6.9)). The plate was incubated at 25 °C for 5 min and the absorbance measured at 405 nm. The inhibition of α-glucosidase activity was expressed in % using the following equation:

$$\% \text{ Inhibition} = \frac{\text{Abs}_{\text{negative control}} - \text{Abs}_{\text{sample}}}{\text{Abs}_{\text{negative control}}} \times 100$$

Statistical analysis

The results were expressed as average ± standard deviation (SD) for each experimental group. Normality was verified using Shapiro Wilk normality test. Comparisons between groups were made using *t*-test. The differences were considered significant at $p<0.05$. GraphPad Prism version 8.0.1 (PRISM GraphPad Software, USA) was used for all comparisons.

Results

Lipid content of *Gelidium corneum* and residue

The total lipid content of *G. corneum* harvested in the summer, obtained using a modified Bligh and Dyer method, was 0.21 ± 0.02 % of dry weight (DW). The lipid content in the *G. corneum* residue obtained after agar extraction was 0.46 ± 0.02 % DW. It was significantly higher than that found in the *G. corneum* biomass ($p<0.0001$). The total content of PL, GL, TG, phenolics, and pigments was also quantified (Fig. 1). Glycolipids were quantified with a significant higher content in *G. corneum* (27.24 ± 0.50 % for *G. corneum* and 3.58 ± 0.32 % for residue, <0.0001), while PL (2.91 ± 0.04 % for *G. corneum* and 4.30 ± 0.27% for residue, $p<0.0009$) and TG content (11.95 ± 1.59 % for *G. corneum* and 25.62 ± 2.03 % for residue, $p<0.0008$) were significant higher in *G. corneum* residue (Fig. 1). The pigments (4.66 ± 0.08 % for *G. corneum* and 1.22 ± 0.01 % for residue, $p<0.0001$) and phenolic compounds (14.04 ± 0.07% for *G. corneum* and 8.78 ± 1.26 % for residue, $p<0.002$) were significantly more abundant in the *G. corneum* lipid extracts, being approximately twice as abundant than in the residue (Fig. 1). Other compounds, such as sphingolipids, betaine lipids, and sterols, contributed with approximately 39.20 ± 1.11 % in the *G. corneum* and were higher in the residue, approximately 56.49 ± 2.87 % (Fig. 1).

Fatty acid profile of *Gelidium corneum* and residue

The esterified FA profile of *G. corneum* and its residue was analyzed by GC-MS after alkaline transmethylation using KOH/methanol. A total of 9 FAs were identified in both *G. corneum* and its residue (Table 1). In *G. corneum*, the most abundant esterified FAs were palmitic acid (FA 16:0, 50.95 ± 3.94%), arachidonic acid (FA 20:4 *n*−6, 13.83 ± 2.15%), stearic acid (FA 18:0, 10.89 ± 6.40%) and oleic acid (FA 18:1 *n*−9, 8.93 ± 4.28%), respectively (Table 1). In *G. corneum* residue, FA 16:0 (34.96 ± 0.75 %), linoleic acid (FA 18:2 *n*−6; 16.60 ± 1.30 %), FA 18:1 *n*−9 (16.44 ± 0.69 %) and FA 18:0 (12.61 ± 1.32 %) were the most abundant esterified FAs (Table 1). Eicosapentaenoic acid (FA 20:5 *n*−3) was also identified in both *G. corneum* samples, with higher levels observed in the *G. corneum* (7.04 ± 1.28 %) compared to the residue (1.17 ± 0.11 %). By comparing the FA profile between *G. corneum* and its residue, we can highlight that *G. corneum* had higher FA 20:4 *n*−6 and FA 20:5 *n*−3 levels, while the residue had higher FA 18:1 *n*−9 and FA 18:2 *n*−6 levels. Overall, in the *G. corneum*, saturated FAs (SFAs), monounsaturated FAs (MUFAs) and PUFAs accounted for 65.91 ± 4.78 %, 11.87 ± 4.13 %, and 22.21 ± 3.42 %, respectively. In the residue, SFAs accounted for

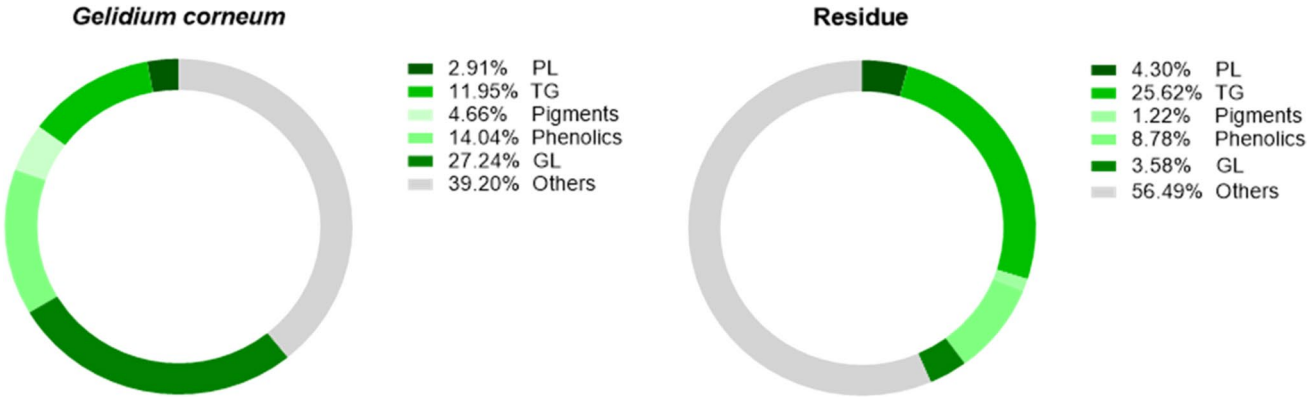

Fig. 1 Lipid composition of *Gelidium corneum* and its residue after agar extraction, including the contents of phospholipids (PL), glycolipids (GL), triacylglycerols (TG), pigments, phenolics and other lipids (including betaine lipids, sterols, sphingolipids as ceramides, hexosylceramides and sulfonolipids and fatty amides lipids) obtained with a modified Bligh and Dyer method. Values are expressed as a percentage (%) of dried lipid extract

Table 1 Fatty acid (FA) profile of the *Gelidium corneum* and its residue obtained after agar extraction analyzed using chromatography–mass spectrometry (GC-MS). Results are expressed in μg mg^{-1} lipid extract and in percentage (%) of total FA. Values are the means of five analytical samples ($n = 5$) ± standard deviation. MUFAs – monounsaturated fatty acids; PUFAs – polyunsaturated fatty acids; SFAs – saturated fatty acids

	μg mg^{-1} lipid extract		% total FA	
Fatty acid	*G. corneum*	Residue	*G. corneum*	Residue
FA 14:0	3.52 ± 0.34	1.01 ± 0.19	4.08 ± 0.76	2.00 ± 0.27
FA 16:0	44.41 ± 2.54	17.42 ± 1.56	50.95 ± 3.94	34.96 ± 0.75
FA 16:1 *n*−7	1.46 ± 0.11	3.8 ± 0.36	1.67 ± 0.18	7.65 ± 0.16
FA 18:0	9.83 ± 6.07	6.29 ± 0.87	10.89 ± 6.40	12.61 ± 1.32
FA 18:1 *n*−9	7.94 ± 3.55	8.19 ± 0.71	8.93 ± 4.28	16.44 ± 0.69
FA 18:1	1.11 ± 0.13	2.87 ± 0.17	1.27 ± 0.14	5.77 ± 0.28
FA 18:2 *n*−6	1.19 ± 0.18	8.26 ± 0.84	1.35 ± 0.09	16.60 ± 1.30
FA 20:4 *n*−6	12.1 ± 1.93	1.39 ± 0.12	13.83 ± 2.15	2.80 ± 0.25
FA 20:5 *n*−3	6.15 ± 1.08	0.58 ± 0.04	7.04 ± 1.28	1.17 ± 0.11
∑ SFAs	57.76 ± 7.58	24.71 ± 2.72	65.91 ± 4.78	49.56 ± 1.49
∑ MUFAs	10.50 ± 3.99	14.87 ± 1.30	11.87 ± 4.13	29.87 ± 0.51
∑ PUFAs	19.44 ± 3.46	10.23 ± 1.30	22.21 ± 3.42	20.57 ± 1.34
∑ *n*−3 PUFAs	6.15 ± 1.21	0.58 ± 0.04	7.04 ± 1.28	1.17 ± 0.11
∑ *n*−6 PUFAs	13.29 ± 2.26	9.66 ± 1.00	15.17 ± 2.14	19.41 ± 1.32

49.56 ± 1.49 %, MUFAs for 29.87 ± 0.51 %, and PUFAs for 20.57 ± 1.34 %, respectively. Among PUFAs, *n*−3 PUFAs were higher in biomass (7.04 ± 1.28 % in *G. corneum* and 1.17 ± 0.11 % in residue), while *n*−6 PUFAs were slightly higher in residue (15.17 ± 2.14 % in *G. corneum* and 19.41 ± 1.32 % in residue) (Table 1).

The FA profile was used to calculate the nutritional quality indicators, namely, the atherogenicity (AI) and thrombogenicity (TI) indexes, and the hypocholesterolemic/hypercholesterolemic (h/H) and *n*−6/*n*−3 PUFAs ratios to evaluate the potential health benefits of FAs from both *G. corneum* and its residue (Table 2). The *G. corneum* showed lowest values for *n*−6/*n*−3 (2.17 ± 0.10) and h/H ratios (0.57 ± 0.10) compared to the residue (16.73 ± 1.68 and 1.00 ± 0.06, respectively). The AI and TI values of *G. corneum* (2.01 ± 0.37 and 1.92 ± 0.40, respectively) were higher than those of the residue (0.85 ± 0.05 and 1.76 ± 0.10, respectively).

Table 2 Nutritional and healthy quality indicators of the lipids from *Gelidium corneum* and its residue. Values are the means of five analytical samples (n=5) ± standard deviation

	Esterified Fatty Acids	
Fatty acid	*G. corneum*	Residue
n−6/*n*−3	2.17 ± 0.10	16.73 ± 1.68
AI	2.01 ± 0.37	0.85 ± 0.05
TI	1.92 ± 0.40	1.76 ± 0.10
h/H	0.57 ± 0.10	1.00 ± 0.06

Lipidomic profile of *Gelidium corneum* biomass and residue

The lipid profile of *G. corneum* and its residue was analyzed by C18-RP-LC-ESI-MS and MS/MS. The characterization

of the lipid profile allowed the identification of 408 lipid species present in *G. corneum* and 432 lipid species present in residue (Table 3 and Tables S1-S9). The lipid species were distributed by 4 lipid groups of polar lipids (PL, GL, sphingolipids (SP) and BT), 2 classes of neutral lipids (diacylglycerol (DG) and triacylglycerol (TG)), 3 fatty acyl amides (*N*-acyl glycine (NAGly), *N*-acyl glycine (NAGly) and *N*-acyl-glycine serine (NAGlySer)), and sterol lipids (ST) (Fig. 2 and Tables S1-S9). The glycerophospholipid (also referred to as PL) classes identified in *G. corneum* and its residue included phosphatidylcholine (PC), lysophosphatidylcholine (LPC), phosphatidylethanolamine (PE), phosphatidylglycerol (PG), phosphatidylinositol (PI), and cardiolipin (CL). Phosphatidic acid (PA), bismonoacylglycerophosphate (BMP), and hemibismonoacylglycerophosphate (HBMP) were only identified in *G. corneum* (Fig. 2 and Tables S1-S4). The GL classes identified in both samples included digalactosyldiacylglycerol (DGDG), monogalactosyldiacylglycerol (MGDG), sulfoquinovosildiacylglycerol (SQDG), glucuronosyldiacylglycerol (GlcADG), acyl monogalactosyldiacylglycerol (acMGDG), acyl digalactosyldiacylglycerol (acDGDG), and acyl glucuronosyldiacylglycerol (acGlcADG) (Fig. 2 and Tables S1-S9). The SP classes identified *G. corneum* and its residue included ceramide (Cer), hexosylceramide (HexCer), ceramide phosphoinositol (PI-Cer), and sulfonolipid (SL) (Fig. 2 and Tables S1-S9). Ceramide phosphoethanolamine (PE-Cer) was only identified in *G. corneum*. Two BT classes were also identified in both samples, namely diacylglyceryl-*N,N,N*-trimethyl homoserine (DGTS) and monoglyceryl-*N,N,N*-trimethyl homoserine (MGTS). The fatty amides lipids, NAGly and NAOrn, were identified in both samples, while NAGlySer was only found in *G. corneum* residue (Fig. 2 and Tables S1-S9). The neutral lipids DG and TG, as well as the ST, were identified in both *G. corneum* samples (Fig. 2).

In *G. corneum*, a total of 290 polar lipid species (53 PL, 102 GL, 13 BT and 122 SP), 11 ST, 4 fatty amides lipids (3 NAGly and 1 NAOrn), and 103 neutral lipids (9 DG and 94 TG) were identified (Fig. 2**;** Tables S1 and S9). In *G. corneum* residue, a total of 299 polar lipid species (69 PL, 66 GL, 10 BT and 154 SP), 12 ST, 8 fatty amides lipids (2 NAGly, 2 NAGlySer and 4 NAOrn), and 113 neutral lipids (10 DG and 103 TG) were identified (Fig. 2; Tables S5 and S9).

In *G. corneum*, the PL classes identified were PC, LPC, PE, PI, PG, PA, CL, BMP and HBMP (Table S1 and Figure S1). Within these classes, several lipid molecular species, including the ones with higher relative abundance in each class (Figure S1), had FA 16:0, FA 20:4 $n-6$ and FA 20:5 $n-3$ (Table S1). On the other hand, in *G. corneum* residue, most of the lipid molecular species within the PL classes PC, LPC, PE, PI, PG, and CL (Table S5 and Figure S1) were esterified with FA 16:0, FA 18:1 $n-9$ and FA 18:2 $n-6$ (Table S5). These results align with the data from FAs analysis (Table 1). The classes of PA, BMP, and HBMP were not identified in the *G. corneum* residue, likely due to their overall lower relative abundance even in *G. corneum*, which may have resulted in their loss during the biomass processing for agar extraction.

Among GL, the classes of MGDG, DGDG, SQDG, GlcADG, acMGDG and acDGDG were identified in both *G. corneum* and its residue, while acGlcADG was only found in *G. corneum* (Figure S2; Tables S1 and S5). Although the GL classes profile was generally similar in both samples in terms of the relative abundance of lipid molecular species within each class, major differences were observed in the MGDG profile (Figure S2A). As for PL classes, MGDG molecular species in *G. corneum* were mostly esterified with FA 16:0, FA 20:4 $n-6$ and FA 20:5 $n-3$ (Table S1), while in its residue FA 16:0 and FA 18:1 $n-9$ were the dominant FAs (Table S5). Additionally, only 64 out of the 102 GL molecular species found in *G. corneum* were detected in its residue. Several GL species containing FA 20:4 $n-6$ and FA 20:5 $n-3$ were found in *G. corneum*, but fewer were identified in the residue. The same trend was also observed for PL. These results agree with the FAs data (Table 1; Figure S3).

The SP classes identified in *G. corneum* and its residue were Cer, HexCer, PI-Cer, PE-Cer (only in *G. corneum*) and SL (Figure S4; Tables S1 and S5). Among them, Cer was the one SP class with the highest diversity in lipid molecular species, comprising different Cer species with different types of long-chain bases (LCBs) and fatty acyl chains (Figure S4A and B; Tables S1 and S5). In most molecular species of Cer in *G. corneum*, 18:0;O3 and 18:1;O3 were the predominant LCBs, while in its residue, 18:0;O2 was also greatly prevalent. The fatty acyl chains in Cer molecular species ranged between C14 and C28, including odd-chain and hydroxylated acyl chains (Tables S1 and S5). The profiles of HexCer, PI-Cer, and SL were comparable, although some differences in the relative abundance of certain species were observed between *G. corneum* and its residue. Specifically, PI-Cer 43:2;O4 and PI-Cer 42:1;O4 were the most abundant PI-Cer in *G. corneum*, each accounting for approximately 25% of the total PI-Cer content. In *G. corneum* residue, the most abundant PI-Cer species were PI-Cer 42:1;O3 and PI-Cer 42:0;O2, each accounting for approximately 18% of total content of this SP class (Figure S4D). For SL class, SL 32:0;O (SL 17:0;O/15:0) and SL 33:0;O2 comprise approximately 40% and 50% of total SL content in *G. corneum* and its residue, respectively (Figure S4F).

The overall composition of BT class DGTS was similar between *G. corneum* and its residue, being mostly composed of FA 16:0 and FA 18:1 $n-9$ (Figure S5; Tables S1 and S5). However, in *G. corneum*, the most abundant lipid molecular species was DGTS 32:1 (DGTS 16:0_16:1), while in residue, it was DGTS 34:1 (DGTS 16:1_18:1), which accounted

Table 3 Lipid classes, total number of lipid species and number of lipid molecular species containing FA 20:5 *n*−3, FA 20:4 *n*−6, FA 18:2 *n*−6, and FA 18:1 *n*−9 within each lipid class, as well as the most abundant lipid molecular species

Gelidium corneum	Biomass						Residue					
	Number of lipid species	Number of Lipid Molecular Species with				Most abundant molecular species	Number of lipid species	Number of Lipid Molecular Species with				Most abundant molecular species
Lipid classes		20:5	20:4	18:2	18:1			20:5	20:4	18:2	18:1	
Glycerophospholipids												
PC	23	0	2	2	1	PC 16:0_20:4, PC 18:2/18:2	26	0	0	4	5	PC 18:2/18:2, PC 18:1_18:2
LPC	6	0	1	0	0	LPC 16:0, LPC 24:0	5	0	0	1	1	LPC 18:2, LC 18:1
PE	3	0	0	0	0	PE 16:0_16:1, PE 31:2	12	0	0	2	5	PE 16:0_16:1, PE 16:1_18:1
PI	2	0	0	1	0	PI 16:0_18:2, PI 34:1	4	0	0	2	1	PI 16:0_18:2, PI 16:0_18:3
PG	10	1	1	1	4	PG 18:1/18:1, PG 16:0/16:0	14	0	0	0	6	PG 16:0_16:1, PG 16:0_18:1
PA	2	0	1	2	0	PA 16:0_20:4, PA 18:2/18:2	-	-	-	-	-	-
CL	2	0	0	0	0	CL 66:2, CL 64:2	8	0	0	0	3	CL 16:1_16:0_16:0_16:1, CL 16:0_16:1_16:1_18:1
BMP	1	0	0	0	0	BMP 16:0/16:0	-	-	-	-	-	-
HBMP	4	2	2	1	1	HBMP 16:0_20:5_16:0, HBMP 16:0_20:5_16:0	-	-	-	-	-	-
Glycerolipids												
MGDG	17	4	4	1	7	MGDG 16:0/16:0, MGDG 16:0_20:4	11	1	1	0	5	MGDG 18:1/18:1, MGDG 16:0/16:0
DGDG	22	1	2	1	8	DGDG 16:0_18:1, DGDG 16:0_20:5	15	1	2	1	6	DGDG 16:0_18:1, DGDG 16:0_20:5
SQDG	14	1	1	0	0	SQDG 30:0, SQDG 16:0/16:0	13	0	1	0	0	SQDG 30:0, SQDG 16:0/16:0
GlcADG	16	0	1	1	5	GlcADG 16:0_18:1, GlcADG 16:0_18:1;O	10	0	0	0	2	GlcADG 16:0_18:1, GlcADG 16:0_18:1;O
acMGDG	10	4	5	1	3	acMGDG 16:0_16:0_18:1, acMGDG 16:0_16:0_20:4	6	0	0	0	1	acMGDG 16:0_16:0_18:1, acMGDG 52:5
acDGDG	19	6	6	2	6	acDGDG 16:0_16:0_18:1, acDGDG 16:0_16:0_20:5	11	1	0	0	3	acDGDG 16:0_16:0_18:1, acDGDG 16:0_16:0_20:5
acGlcADG	4	1	1	0	3	acGlcADG 16:0_18:1_16:0, acGlcADG 16:0_18:1_18:1	-					
Betaine lipids												
DGTS	1	0	0	1	5	DGTS 16:0_16:1, DGTS 16:1_18:1	1	0	0	0	3	DGTS 16:1_18:1, DGTS 16:0_18:1
MGTS	12	0	0	0	0	MGTS 16:0	9	0	0	0	0	MGTS 16:0
Sphingolipids												
Cer	94	0	0	0	0	Cer 18:1;O3/24:0;O, Cer 18:1;O3/24:1;O	123	0	0	0	0	Cer 18:0;O3/24:1;O, Cer 18:1;O3/24:1;O
HexCer	10	0	0	0	0	HexCer 18:1;O3/25:1;O, HexCer 18:0;O3/24:1;O	11	0	0	0	0	HexCer 18:1;O3/25:1;O, HexCer 18:1;O3/24:0;O

Table 3 (continued)

Gelidium corneum	Biomass						Residue					
	Number of lipid species	Number of Lipid Molecular Species with				Most abundant molecular species	Number of lipid species	Number of Lipid Molecular Species with				Most abundant molecular species
Lipid classes		20:5	20:4	18:2	18:1			20:5	20:4	18:2	18:1	
PI-Cer	14	0	0	0	0	PI-Cer 42:1;O3, PI-Cer 42:0;O2	12	0	0	0	0	PI-Cer 42:1;O3, PI-Cer 42:1;O4
PE-Cer	1	0	0	0	0	PE-Cer 34:2;O2	-	0	0	0	0	-
SL	3	0	0	0	0	SL 17:0;O/17:0;O, SL 17:0;O/15:0	8	0	0	0	0	SL 33:0;O2, 17:0;O/15:0
Sterol lipids												
ST	11	0	0	0	0	ST 27:3;O, ST 28:4;O2_1	12	0	0	0	0	ST 27:3;O, ST 28:4;O2_2
Neutral lipids												
DG	9	1	4	2	2	DG 20:4/20:4, DG 16:0_20:4	10	2	3	3	4	DG 18:3/18:3, DG 20:4/20:4
TG	94	4	9	12	25	TG 16:0_20:4_20:4, TG 60:12	103	1	4	25	19	TG 16:0_18:2_18:2, TG 18:1_18:2_18:3
Fatty amides												
NAGly	3	0	0	0	0	NAGly 16:0;O(FA 15:0), NAGly 17:0;O(FA 17:1)	2	0	0	0	0	NAGly 16:0;O(FA 15:0), NAGly 17:0;O(FA 15:0)
NAGlySer	-	-	-	-	-	-	2	-	-	-	-	NAGlySer 32:1;O2, NAGlySer 32:2;O2
NAOrn	1	0	0	0	0	NAOrn 18:1;O(FA 16:0)	4	0	0	0	0	NaOrn 36:3;O2, NaOrn 32:1;O2

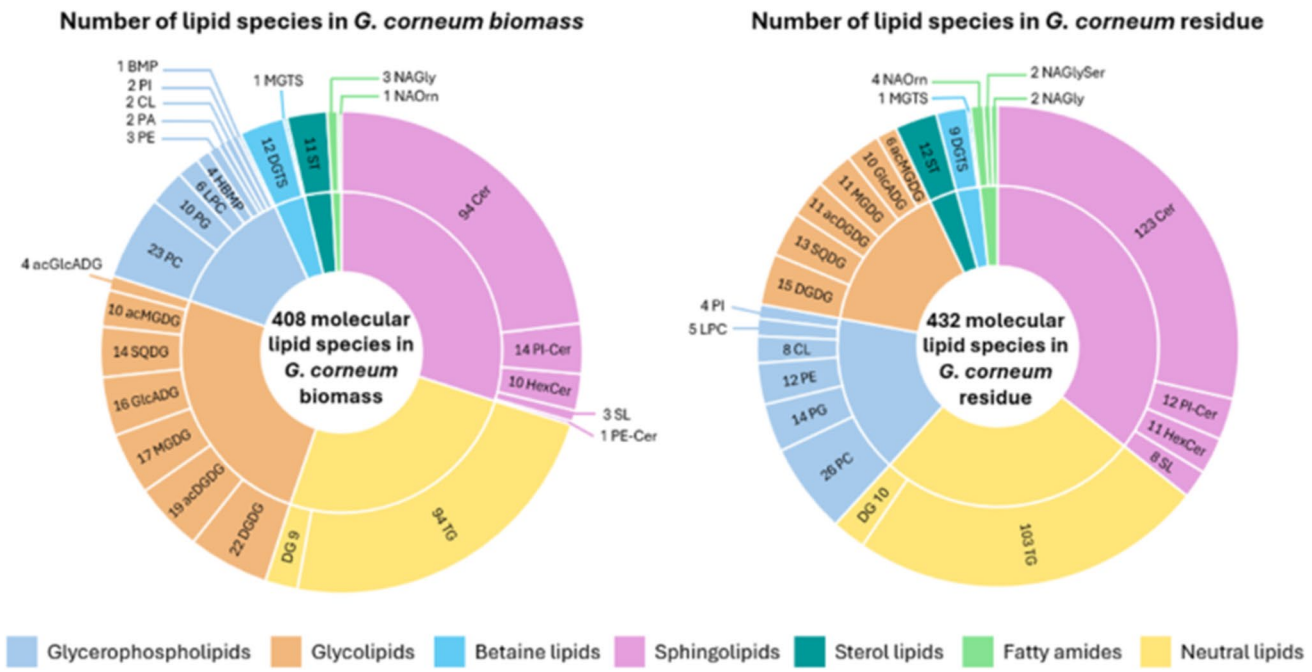

Fig. 2 Number of lipid species identified in *Gelidium corneum* and its residue using C18-RP-LC-ESI-MS/MS. acDGDG – acyl digalactosyldiacylglycerol; acGlcADG – acyl glucuronosyldiacylglycerol, acMGDG – acyl monogalactosyldiacylglycerol; BMP – bis(monoacylglycero)phosphates; Cer – ceramide; CL – cardiolipin; DG – diacylglicerol; GlcADG – glucuronosyldiacylglycerol; DGDG – digalactosyldiacylglycerol; DGTS - diacylglyceryl-*N,N,N*-trimethyl homoserine; HBMP – hemibismonoacylglycerophosphate; HexCer – hesoxylceramide; LPC – lyso phosphatidylcholine; MGDG – monogalactosyldiacylglycerol; MGTS – monoacylglyceryl-*N,N,N*-trimethyl homoserine; NAGly – *N*-acyl glycine; NAGlySer – *N*-acyl glycyl serine; NAOrn – *N*-acyl ornithine; PA – phosphatidic acid; PC – phosphatidylcholine; PE – phosphatidylethanolamine; PG – phosphatidylglycerol; PI – phosphatidylinositol; PE-Cer – ceramide phosphoethanolamine; PI-Cer – ceramide phosphoinositol; SL – sulfonilipid; SQDG – sulfoquinovosyldiacylglycerol; ST – sterol lipid; TG – triacylglicerol

for approximately 50% and 36% of the total DGTS content in each *G. corneum* sample, respectively (Figure S5A). Additionally, only MGTS 16:0 was identified in both samples (Figure S5B). Among fatty acyl amides, NAGly (Figure S5C) and NAOrn (Figure S5E) were identified in both *G. corneum* samples, while NAGlySer (Figure S5D) was only found in *G. corneum* residue.

The profile of lipid molecular species of DG class was also quite similar between *G. corneum* samples with lipid molecular species composed of FA 16:0, FA 18:1 *n*−9, FA 18:2 *n*−6, FA 18:3, FA 20:4 *n*−6 and FA 20:5 *n*−3, although the most abundant lipid molecular species differed (Figure S6; Tables S1 and S5). In *G. corneum*, DG 40:8 (DG 20:4/20:4) accounted for 50% of the total DG content, while in the residue, DG 36:6 (18:3/18:3) comprised 30% of the total DG content (Figure S6A). Regarding the TG profile, around 100 lipid species were found in *G. corneum* samples (Figure S6; Tables S1 and S5). The FA composition of TG molecular species in *G. corneum* included FA ranging from FA 6:0 to FA 26:0 (Table S1), while in its residue, the range was from FA 6:0 to FA 25:0 (Table S5). Interestingly, FA with 18 and 20 carbons exhibited varying degrees of unsaturation, ranging from 1 to 5. In *G. corneum*, TG 56:8_2 (TG 16:0_20:4_20:4) accounted for 11% of the total TG content, being the most abundant TG species (Figure S6B and C). On the other hand, TG 52:4 (TG 16:0_18:2_18:2) and TG 54:6 (18:1_18:2_18:3) were the most abundant in *G. corneum* residue, each accounting for approximately 8% of total TG content (Figure S6 B and C).

Several ST were also identified in both *G. corneum* samples (Figure S6D; Tables S1 and S5), with ST 27:3;O (40% of total ST content) and ST 28:4;O2_1 (24% of total ST content) most abundant in *G. corneum* and ST 27:3;O (47% of total ST content) and ST 28:4;O2_2 (22% of total ST content) in the residue.

Overall, the lipid profile of *G. corneum* and its residue exhibit both similarities and differences (Tables S1, S5 and S9). A total of 345 lipid species were similar in both samples, while 63 and 87 lipid species were identified only in *G. corneum* and its residue, respectively (Figure S3).

Screening of biological activities

Antioxidant activity

The antioxidant potential of lipids from *G. corneum* biomass and residue was evaluated using the ABTS$^{\bullet+}$ and DPPH$^{\bullet}$

scavenging assays after 120 min of reaction. For $ABTS^{\bullet+}$ assay, the percentage of scavenging at 50, 100 and 250 µg mL^{-1} was 9.66 ± 0.86 %, 21.33 ± 1.37 %, and 36.52 ± 1.16 % for *G. corneum* and 8.03 ± 1.47 %, 14.90 ± 2.02 %, and 34.41 ± 1.82 % for its residue (Fig. 3A). Lipids from *G. corneum* and its residue were able to scavenge $ABTS^{\bullet+}$ with a SC_{30} of 202.54 ± 4.52 µg mL^{-1} and 216.77 ± 8.84 µg mL^{-1}, and TE of 52.6 ± 1.18 µmol Trolox/g lipid and 49.54 ± 2.08 µmol Trolox g^{-1} lipid, respectively (Table 4). In the $DPPH^{\bullet}$ assay, the scavenging potential was less pronounced, with lipids from *G. corneum* showing 5.92 ± 2.00 %, 10.14 ± 0.91 %, and 14.13 ± 1.17 % of radical scavenging at 50, 100 and 250 µg mL^{-1}, respectively, while its residue provided 5.46 ± 0.40 %, 7.35 ± 0.00 %, and 8.03 ± 1.54 % at the same concentrations (Figure 3A). A SC_{10} of 110.45 ± 6.17 µg mL^{-1} and TE of 40.41 ± 2.35 µmol Trolox g^{-1} lipid was obtained for lipids from *G. corneum*, while for the residue, $DPPH^{\bullet}$ scavenging of less than 10% was observed at the highest concentration (250 µg mL^{-1}) (Fig. 3B).

Anti-inflammatory activity

Lipids from *G. corneum* and its residue showed anti-inflammatory potential by inhibiting the activity of COX-2 between 30% to 80% (Fig. 3). The lipids from *G. corneum* demonstrated a great potential to inhibit COX-2 even at the lowest concentration (69.96 ± 16.57 %, 76.83 ± 2.02 % and 71.52 ± 6.94 % for the 50, 100 and 250 µg mL^{-1}, respectively), with statistically significant differences between the two samples at both 50 µg mL^{-1} ($p < 0.05$) and 100 µg/mL ($p < 0.05$; Fig. 3). A dose-dependent inhibitory effect was observed for lipids from *G. corneum* residue (34.21 ± 10.74 %, 48.37 ± 14.96 % and 63.18 ± 10.66 % for the 50, 100 and 250 µg mL^{-1}, respectively) with an IC_{50} of 155.80 ± 67.60 % (Fig. 3).

Table 4 Trolox equivalents (TE; µmol Trolox g^{-1} lipid), SC_{30} values (µg mL^{-1}) obtained for the $ABTS^{\bullet+}$ assay and SC_{10} (µg mL^{-1}) obtained for the $DPPH^{\bullet}$ assay after 2 h of reaction using different concentrations (50, 100, and 250 µg mL^{-1} in ethanol) of lipid extracts from *Gelidium corneum* and its residue

	$ABTS^{\bullet+}$ assay		$DPPH^{\bullet}$ assay	
	SC_{30}	TE	SC_{10}	TE
G. corneum	202.54 ± 4.52	52.6 ± 1.18	110.45 ± 6.17	40.41 ± 2.35
Residue	216.77 ± 8.84	49.54 ± 2.08	---	---

Antidiabetic activity

The antidiabetic activity of lipids from *G. corneum* and its residue was evaluated using α-amylase and α-glucosidase enzymes (Fig. 3). Lipids from both *G. corneum* samples showed no inhibitory potential against α-amylase at any of the tested concentrations (50, 100 and 250 µg mL^{-1}) but were able to inhibit α-glucosidase activity (Fig. 3). The inhibitory potential increased in a concentration-dependent

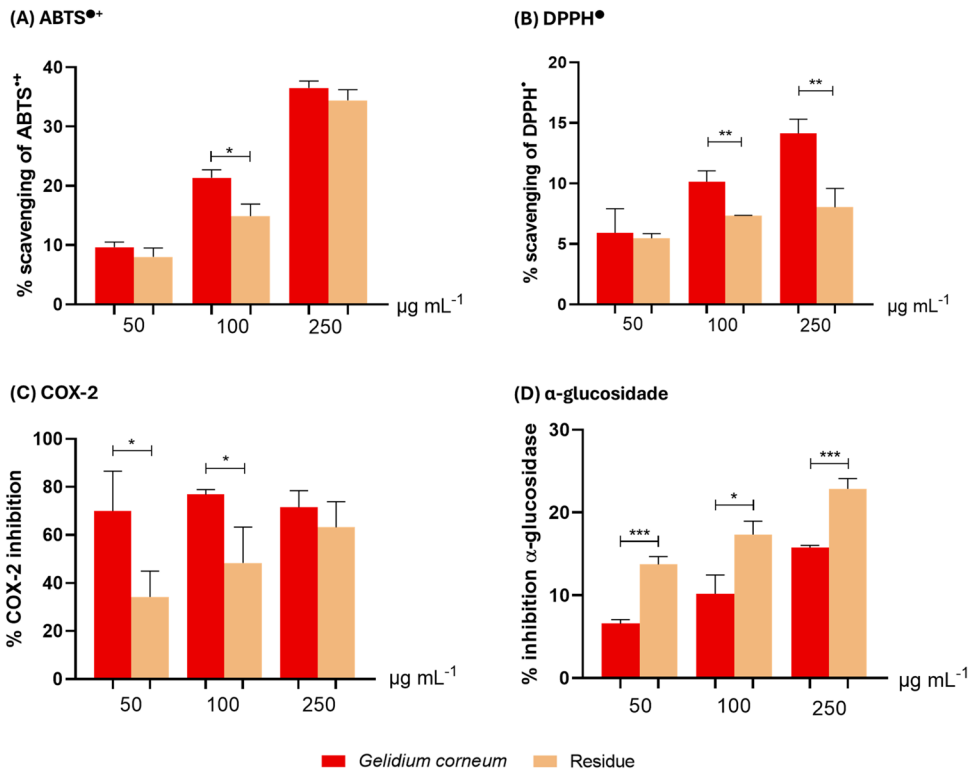

Fig. 3 Biological activities of lipid extracts from *Gelidium corneum* and its residue. Three different concentrations were evaluated (50, 100, and 250 µg/mL). **(A)** Scavenging of 2,2'-azino-bis(3-ethylbenzothiazoline-6-sulfonic acid radical cation ($ABTS^{\bullet+}$); **(B)** Scavenging of 2,2-diphenyl-1-picrylhydrazyl radical ($DPPH^{\bullet}$); **(C)** Inhibition of cyclooxygenase (COX-2) activity; and **(D)** Inhibition of α-glucosidase activity. All results are expressed in percentage (%) and values are average of three assays (n=3) ± standard deviation (SD). Statistical analysis was performed using t-test (*** $p < 0.001$, ** $p < 0.01$, * $p < 0.05$)

manner. Lipids from the residue showed the highest inhibition percentage, reaching 13.75 ± 0.94 % at 50 µg mL^{-1}, 17.33 ± 1.65 % at 100 µg mL^{-1}, and 22.87 ± 1.24 % at 250 µg mL^{-1}, while lipids from *G. corneum* achieved 6.6 ± 0.47 % ($p < 0.001$ *vs* residue), 10.18 ± 2.28 % ($p < 0.05$ *vs* residue), and 15.77 ± 0.27 % ($p < 0.001$ *vs* residue) at 50, 100 and 250 µg mL^{-1} (Fig. 3). In comparison with that, acarbose (positive control) inhibited α-glucosidase activity by 86.43 ± 1.13 % (Figure S7).

Discussion

The *G. corneum* and its residue exhibited a low lipid content, which aligns with observations for other red seaweeds, where the lipid content is known to be low (Freitas et al. 2022). Previous studies also reported a low content of lipids in *G. corneum* (Gomes-Dias et al. 2020; Vega et al. 2020; Cavaco et al. 2021; Mateus et al. 2024), ranging from 0.7 ± 0.1 % using Folch method (Cavaco et al. 2021; Mateus et al. 2024) to 1.16 ± 0.21 % using Soxhlet extraction (Tůma et al. 2020) and 1.47 ± 0.15 % DW using Bligh and Dyer method (Gomes-Dias et al. 2020). However, the lipid content of *G. corneum* observed in this study was lower than that reported in the previous studies. These differences may be attributed to variations in biomass processing conditions or the lipid extraction methods employed (Li et al. 2014). Storage conditions of seaweed biomass, such as fresh, dry, and frozen, as well as biomass pretreatments, can also influence the lipid content due to lipid oxidation and the loss of PUFA (Harrysson et al 2021). Nonetheless, changes in the lipid content with seasonality were also shown, with the lowest lipid content being achieved in winter and summer (0.93 ± 0.04 % DW and 2.16 ± 0.10 % DW, respectively) and the highest in spring (2.75 ± 0.28 % DW) (Cavaco et al. 2021). In fact, whether in wild populations or in aquaculture, local environmental conditions along with other factors, such as nutrient availability or salinity, can impact the lipid content and composition in seaweeds (Moreira et al. 2021). The lipid content of *G. corneum* residue reported in the literature ranges from 0.7 ± 0.1 % (Mateus et al. 2024) to 2.1 ± 0.2 % DW using Folch extraction (Ferreira et al. 2024), 0.87 ± 0.09 % DW using the Bligh and Dyer extraction (Trigueros et al. 2021a), and 3.36 % DW using Soxhlet extraction (Tůma et al. 2020). The lipid content of both *G. corneum* and industrial residues was notably higher when using enzyme-assisted extraction (8.0 ± 0.3 % DW for *G. corneum* and 7.0 ± 0.4 % DW for residue) (Mateus et al. 2024).

Gelidium corneum is a well-known primary source of high-quality agar, with the residue being obtained after agar extraction under extremely harsh conditions that require alkaline pre-treatment followed by boiling seaweed in excess of water (Lebbar et al. 2018; Gomes-Dias et al. 2024). This may lead to the degradation of GL, explaining the lower GL content obtained in *G. corneum* residue. A previous study showed that the alkaline extract of this seaweed contains glycerol-galactosides derivatives, reinforcing the potential degradation of GL during agar extraction (Lebbar et al. 2018). The decrease in pigments and phenolic compounds can also be explained by their degradation with biomass processing to extract high-quality agar (Martínez-Sanz et al. 2019). The reduction in GL, pigments and phenolic compounds in the residue may also result from their extraction during agar preparation, such as rinsing steps following alkaline treatment, or co-extraction with agar, particularly in protocols that omit alkaline pre-treatments, as these are associated with increased co-extraction of non-agar components (Martínez-Sanz et al. 2019; Martínez-Sanz et al. 2021; Pereira et al. 2021).

The results gathered for the FAs profile of *G. corneum* are consistent with previous studies, although the literature also reports the presence of other less abundant FAs (Cavaco et al. 2021). Our results align with earlier studies showing that FA 16:0 is the most abundant FA in *G. corneum*, while FA 20:5 *n*−3 and FA 20:4 *n*−6 were the most abundant *n*−3 FA and *n*−6 FA, respectively (Matos et al. 2020; Cavaco et al. 2021). However, the levels of FA 20:5 *n*−3 and FA 20:4 *n*−6 in this study were lower than those reported by Cavaco et al. (2021), despite both studies analyzing the FA profile of *G. corneum* collected in summer. Although the same alga species and season were considered, the biomass in our study was likely harvested in a different year. It may also have been collected during different summer month or from a different location along the Portuguese coast. Additionally, differences in pre-processing and storage conditions, lipid extraction methods, and FA derivatization and analysis protocols could explain the differences observed in FA 20:5 *n*−3 and FA 20:4 *n*−6 levels. Also, the high proportion of SFAs was previously reported, followed by PUFAs and MUFAs, which account for approximately 20% and <13% of the total FA, respectively (Matos et al. 2020). However, the only study found in literature reports differing results for the FAs composition of *G. corneum* residue (Ferreira et al. 2024). Although EPA remained the most abundant *n*−3, comprising 16.5 ± 0.2 % of total FA, other *n*−3 PUFAs such as α-linolenic acid (FA 18:3 *n*−3; 3.8 ± 0.1 % of total FA) and docosahexaenoic acid (FA 22:6 *n*−3, DHA; 3.7 ± 0.4 % of total FA) were also described in the literature for the residue, though absent in our study. Additionally, the most abundant FA was FA 20:4 *n*−6 (37.1 ± 0.7 % of total FA), followed by FA 16:0 (21 ± 4 % of total FA) (Ferreira et al. 2024). These differences may be attributed to the different lipid analysis methodologies namely for lipid extraction and FAs analysis, or to seasonal variations in the FAs composition of *G. corneum*, as reported previously (Cavaco et al. 2021).

The FA 20:5 *n*−3 is widely recognized for its health benefits, encompassing both its nutritional value and bioactive properties (Avallone et al. 2019; Nassar et al. 2023), and FA 20:4 *n*−6 is a precursor of several biologically active lipid mediators, with important biological functions in health and disease (Wang et al. 2021). Although these two PUFAs can be endogenously converted from α-linolenic acid (FA 18:3 *n*−3) and FA 18:2 *n*−6, respectively, the conversion rate is generally poor, making dietary intake an important source for both (Djuricic and Calder 2023; Kim and Song 2024). FA 18:2 *n*−6, found in higher levels in the *G. corneum* residue, is an essential FA that must be acquired from the diet. This FA is the most abundant *n*−6 FA in the human body and is essential for maintaining health when consumed moderately (Risé et al. 2013). It has been associated with improved cardiovascular risk and reduced incidence of cardiovascular diseases (Marangoni et al. 2020), enhanced long-term glycemic control and insulin resistance (Marangoni et al. 2020) and the attenuation of neuroinflammation (Kim and Song 2024). This FA is also the most abundant PUFA in the skin, being commonly incorporated into cosmetic products for its moisturizing, anti-inflammatory, photoprotective, or skin barrier repair properties, among other benefits (Wang et al. 2025). The *G. corneum* and its residue contain similar levels of FA 18:1 *n*−9, which is recognized as the major contributor to reducing cardiovascular risk, atherosclerosis and hypertension, such as by lowering blood lipid level, and is also implicated in the cardioprotective effects associated with the Mediterranean diet (Lu et al. 2024). Furthermore, this FA is also recognized for its role in regulating cutaneous homeostasis, as well as for its antioxidant and anti-inflammatory properties in many skin diseases, being also used in cosmetic products as emulsifying, emollient and moisturizing ingredient (Atef et al. 2022).

The *G. corneum* showed the lowest values for *n*−6/*n*−3 ratio, although these values were higher than those previously reported, which were consistently close to 1 (Cavaco et al. 2021). The *n*−6/*n*−3 ratio assesses the balance between pro-inflammatory/anti-inflammatory precursors, with a *n*−6/*n*−3 ratio between 1:1 to 5:1 being recommended to maintain a healthy balance (Gonzalez-Becerra et al. 2023). Therefore, a balanced diet in *n*−6/*n*−3 PUFAs can improve life quality and help to prevent inflammation and cardiovascular and nervous system disorders (Yang et al. 2023). The AI and TI values of *G. corneum* and residue were consistent with previously reported ranges for *G. corneum*, with AI values ranged from 0.93 ± 0.01 to 2.89 ± 0.09 and TI values from 0.60 ± 0.01 to 2.54 ± 0.05 (Cavaco et al. 2021). The AI and TI are associated with cardiovascular risk, namely the atherogenic plaques, blood clots development and thrombus formation (Badimon et al. 2012; Tilami and Kouřimská 2022). Lower levels of AI and TI are beneficial to human health, correlated with a higher cardiovascular protective effect (Tilami and Kouřimská 2022). The h/H ratio was higher in the residue than the *G. corneum*. The h/H ratio, linked to PUFAs content, is an important indicator for human health, measuring the effects of FAs composition on cholesterol, with higher value being more beneficial (Chen and Liu 2020). These values were very similar to those previously reported for the *G. corneum*, ranging from 0.35± 0.01 to 1.08 ± 0.01 (Cavaco et al. 2021).

The nutritional quality indicators values of *G. corneum*, particularly the *n*−6/*n*−3 ratio, AI, and TI values, were generally higher than those reported for other red seaweeds, with values consistently ≤1 (Kumar et al. 2011; Paiva et al. 2016; da Costa et al. 2017; da Costa et al. 2018; Susanto et al. 2019; Chen and Liu 2020; Lopes et al. 2020; Costa et al. 2021). These differences can be attributed to the higher levels of esterified SFAs and lower levels of esterified PUFA, particularly FA 20:5 *n*−3, in *G. corneum*. However, while the *n*−6/*n*−3 ratio in *G. corneum* were within the range reported for *Gracilaria gracilis* (*n*−6/*n*−3 ratio of 2.5) (Lopes et al. 2020), it was lower than those reported for *Gracilariopsis longissima* (*n*−6/*n*−3 ratio of 7.69) (Susanto et al. 2019), *Gracilaria* sp. (*n*−6/*n*−3 ratio of 3.6) (da Costa et al. 2017), or *Amphiora anceps* (*n*−6/*n*−3 ratio of 3.37), *Gracilaria corticate* (*n*−6/*n*−3 ratio of 12.35), *Gracilaria dura* (*n*−6/*n*−3 ratio of 27.65), *Gracilaria debilis* (*n*−6/*n*−3 ratio of 18.82), *Gracilaria fergusonii* (*n*−6/*n*−3 ratio of 18.65), *Gracilaria salicornia* (*n*−6/*n*−3 ratio of 3.93), and *Sarconema filiforme* (*n*−6/*n*−3 ratio of 3.48) (Kumar et al. 2011). Similar AI and TI values were reported for *G. longissima* (AI of 2.03 ± 0.24) (Susanto et al. 2019) or *Gelidium micropterum* (TI of 1.83) and *A. anceps* (TI of 2.07) (Kumar et al. 2011), respectively. In contrast, higher AI values were reported for *G. salicornia* (AI of 2.87) (Kumar et al. 2011), while higher TI values were observed for *G. longissima* (TI of 2.80 ± 0.25) (Susanto et al. 2019) as well as for *G. fergusonii* (TI of 2.66) and *G. salicornia* (TI of 5.75) (Kumar et al. 2011). *Gelidium corneum* exhibits lower h/H values compared to those determined from the FAs profile of other red macroalgae (Kumar et al. 2011; Paiva et al. 2016; Chan and Matanjun 2017; da Costa et al. 2017; da Costa et al. 2018; Susanto et al. 2019; Chen and Liu 2020; Lopes et al. 2020; Costa et al. 2021), with h/H only comparable to *G. longissima* (h/H of 0.44 ± 0.03) (Susanto et al. 2019). *Gelidium corneum* exhibited an *n*−6/*n*−3 ratio lower than those reported for common vegetable oils, including sunflower oil, soybean oil, sesame oil, and olive oil, as well as lower than that of palm oil, avocado seed oil and traditional nuts such as hazelnuts, walnuts, or almonds (*n*−6/*n*−3: 6.67-149) (Tilami and Kouřimská 2022). Although the AI and TI values for *G. corneum* were higher than those reported for common vegetable oils, both were like those reported for palm oil (AI and TI of 1.88)

(Tilami and Kouřimská 2022). The h/H ratio of *G. corneum* was lower than a variety of fish oils (h/H: 0.67–8.03) (Dongho Dongmo et al. 2024), fish (h/H: 0.87–4.83), and shellfish (h/H: 1.73–4.75) (Chen and Liu 2020). These vegetable and marine oils rich in omega-3, omega-6, or omega-9 FAs are extensively used as ingredients in food and cosmetic industries. Therefore, these findings emphasize the potential of *G. corneum* as a sustainable source of healthy lipids for foods and cosmetic products.

The lipid profiling of *G. corneum*, and its residue, can contribute to the identification of lipids with nutritional value as well as bioactive and functional properties with promising biotechnological applications. Although the lipid profile of *G. corneum* has not yet been fully characterized, the lipid composition of *Gelidium amansii,* collected from the coastal area in north China, was characterized using reversed-phase liquid chromatography coupled with quadrupole time-of-flight mass spectrometry (RPLC-Q-TOF-MS/MS) (Song et al. 2023). Among the 18 lipids classes found in *G. amansii*, which included a total of 502 lipid species, only the GL class monogalactosylmonoacylglycerol (MGMG) was not detected in *G. corneum*. However, of the 28 lipid classes identified in *G. corneum*, LPC, PA, CL, BMP, HBMP, PI-Cer, PE-Cer, SL, ST, NAGly, and NAOrn were not reported in *G. amansii*. Glycolipids were the predominant components, and its classes accounted for the largest number of lipid species identified in *G. amansii* (Song et al. 2023), whereas in *G. corneum*, SP classes, particularly Cer bearing both LCB 18:0;O3 and 18:1;O3, were more predominant. When comparing the lipid profile of *G. corneum* with that of other red seaweeds, such as *Palmaria palmata* (Lopes et al. 2019a)*, Grateloupia turuturu* (Costa et al. 2021)*, Gracilaria* sp. (da Costa et al. 2017)*, Porphyra dioica* (da Costa et al. 2018) and *Chondrus crispus* (Melo et al. 2015), it is evident that these species share several common lipid classes, including PC, LPC, PE, PG, PI, PA, PI-Cer, HexCer, DGDG, MGDG, SQDG, DGTS and MGTS classes. However, Cer, PE-Cer, BMP, HBMP, GlcADG, acMGDG, acDGDG, acGlcADG, SL, ST, NaGly and NaOrn have not yet been reported in these species. However, all shared several lipid species bearing FA 20:4 *n*−6 and FA 20:5 *n*−3 (Melo et al. 2015; da Costa et al. 2017; da Costa et al. 2018; Lopes et al. 2019a; Costa et al. 2021).

Unveiling the specificity of the lipid composition of *G. corneum* and its residue will be valuable for targeting specific compounds of interest with industrial applications, contributing to the circular bioeconomy and blue growth, while also supporting zero-waste goals. Among the observed differences in the lipid profiles of *G. corneum* and its residue, we can highlight the reduction in the number of GL molecular species found in the residue. This high reduction is consistent with the low GL amounts observed in this sample, reinforcing the traces contents in these lipids and possible degradation of GL during agar extraction. In fact, it is well established that carbohydrates degrade under alkaline conditions (Berglund et al. 2019). Nevertheless, the possibility of GL extraction during agar preparation cannot be excluded. Furthermore, fewer GL and PL molecular species containing FA 20:4 *n*−6 and FA 20:5 *n*−3 were found in the residue, indicating that lipid species bearing these PUFA may have a higher susceptibility for degradation during biomass processing for agar extraction. The lipid species identified exclusively in *G. corneum* include several polar lipids containing highly unsaturated FA, namely FA 20:4 *n*−6 and FA 20:5 *n*−3. These lipid species include the phospholipids PC 40:9, LPC 20:4, PG 36:4, PG 36:5, HBMP 52:4, HBMP 52:5, HBMP 56:9, and PA 40:8, as well as the glycolipids SQDG 38:5, MGDG 38:5, MGDG 38:6, MGDG 40:8, MGDG 40:10, DGDG 34:4, DGDG 36:5;O, DGDG 36:5;2O, GlcADG 36:4, acGlcADG 54:5, acGlcADG 54:6, acMGDG 54:6, acMGDG 56:10, acMGDG 60:14, acDGDG 50:5;O, acDGDG 52:6, acDGDG 56:8, acDGDG 56:10. This supports the FA results, in which the residue showed lower levels of FA 20:4 *n*−6 and FA 20:5 *n*−3 compared to *G. corneum*.

PL and GL molecular species bearing FA 20:4 *n*−6 and FA 20:5 *n*−3 were more abundant in *G. corneum*, while the ones with FA 18:1 *n*−9 and FA 18:2 *n*−6 were higher in the residue. Additionally, DG and TG species bearing these FA were also identified in both *G. corneum* samples. FA 18:1 *n*−9 and FA 18:2 *n*−6 are primarily sourced from vegetable oils, seeds, and nuts (Liu et al. 2023; Kim and Song 2024). On the other hand FA 20:4 *n*−6 is found in meat, fish, dairy products or eggs (Kawashima 2019), and FA 20:5 *n*−3 is mainly derived from fatty fish, fish oils, and nutritional supplements (Djuricic and Calder 2023; Liu et al. 2023). Furthermore, when *n*−3 PUFAs are esterified in polar lipids, they appear to be more bioavailable and biologically active (Navarro López et al. 2023). Given this, *G. corneum* and particularly its residue represents a promising and sustainable source of nutritional and healthy lipids, offering a solution to reduce environmental and economic impacts associated with the overexploitation of arable land, deforestation of crop plantations, and the depletion of fish stocks due to overfishing. Therefore, lipids from *G. corneum* samples represent a natural source of ingredients with high nutritional value and health benefits for use in food and nutraceutical industries.

Additionally, lipids from *G. corneum* samples, specially the residue, can also be used to produce natural lecithin, a blend of various lipids including TG, FA, sterols, GL, SP and PL, all present in *G. corneum*, which are highly valued across multiple industrial sectors, including food and cosmetics (Alhajj et al. 2020). Among the lipids identified in *G. corneum* samples, the Cer profile shown both the LCB and long-chain SFA, as well as hydroxylated and odd chain-FA,

which are commonly found in skin cells (Hinder et al. 2011; Kawana et al. 2020; Knox and Boyle 2021). This emphasizes the potential value of lipids from this seaweed for cosmetics industry, particularly from residue where the fractions that include SP, particularly Cer, are higher. Therefore, lipids from *G. corneum* can be used as emulsifiers (e.g., PLs), flavor or fragrance carriers (e.g., TG), texturizer agents (e.g., TG), preservative agents (e.g., glycerolipids, SP), bioactive ingredient delivery systems (e.g., PL), as well as active ingredients (e.g., glycerolipids, SP, sterols), among other applications (De Luca et al. 2021; Ahmad et al. 2025).

Since lipids can be used as active ingredients, in this study we evaluated the antioxidant, anti-inflammatory and anti-diabetic properties of lipids from *G. corneum* and its residue. The results from antioxidant activity suggested that lipids from *G. corneum* and its residue scavenged both radicals in a concentration-dependent manner, with lipids from *G. corneum* exhibiting higher radical-scavenging potential, although both showing greater scavenging against $ABTS^{\bullet+}$ compared to $DPPH^{\bullet}$. However, the synergistic effect between lipids, pigments, and phenolic compounds, the latter two with well-established antioxidant properties (Safafar et al. 2015; Lu et al. 2021) and present in higher amounts in *G. corneum*, should not be disregarded to explain the observed overall antioxidant activity. Additionally, $ABTS^{\bullet+}$ assay enables the screening of both lipophilic and hydrophilic bioactive compounds, resulting in generally higher scavenging activity than in the $DPPH^{\bullet}$ assay (Munteanu and Apetrei 2021). Compared with other red seaweeds, such as *G. gracilis* ($ABTS^{\bullet+}$: IC_{50} 86.4 ± 3.4 μg mL^{-1}, TE 183.0 ± 7.1 μmol of Trolox g^{-1} lipid and $DPPH^{\bullet}$: IC_{20} 119.6 ± 1.8 μg mL^{-1}, TE 89.2 ± 1.3 μmol of Trolox/g lipid) (Lopes et al. 2020), *P. palmata* ($ABTS^{\bullet+}$: IC_{50} 23.7 ± 0.6 μg mL^{-1}, TE 606.1 ± 14.6 μmol of Trolox g^{-1} lipid and $DPPH^{\bullet}$: IC_{20} 119.6 ± 1.8 μg mL^{-1}, TE 89.5 ± 6.3 μmol of Trolox g^{-1} lipid) (Lopes et al. 2020), *P. dioica* ($ABTS^{\bullet+}$: IC_{50} 41.1 ± 2.5 μg mL^{-1}, TE 41.1 ± 2.5 μmol of Trolox g^{-1} lipid and $DPPH^{\bullet}$: IC_{20} 212.5 ± 7.0 μg mL^{-1}, TE 44.9 ± 1.5 μmol of Trolox g^{-1} lipid) (Lopes et al. 2020), and *G. turuturu* ($ABTS^{\bullet+}$: IC_{50} 130.4 ± 52.4 μg mL^{-1}, TE 7.3 ± 3.7 μmol of Trolox g^{-1} lipid and $DPPH^{\bullet}$: IC_{25} 129.1 ± 58.7 μg mL^{-1}, TE 83.2 ± 39.6 μmol of Trolox g^{-1} lipid) (Costa et al. 2021), lipids from *G. corneum* seems to exhibit lower antioxidant potential. Indeed, a previous study reported that, despite the high content in polyphenols typically associated with strong antioxidant properties, the ethanolic extracts from *G. corneum* also harvested from the Portuguese Coast exhibited low antioxidant activity to scavenge $DPPH^{\bullet}$, with inhibition levels of 6.8 ± 1.2 % (Matos et al. 2020). The $DPPH^{\bullet}$ scavenging ability of other extracts from *G. corneum* collected in Portugal Coast and with relatively high phenolic content was also evaluated, yielding EC_{50} values ranging from 399.60 μg mL^{-1} to 991.60 μg mL^{-1} (Matias et al. 2023). Ethanolic extracts (70% ethanol) from *G. corneum* collected from the Moroccan Atlantic Ocean exhibited highest antioxidant potential (IC_{50} 84.61 ± 3.9 mg mL^{-1} in $DPPH^{\bullet}$ assay; IC_{50} 44.46 ± 2.4 mg mL^{-1} in $ABTS^{\bullet+}$ assay) (Grina et al. 2020), suggesting that geographic location may influence the profile of antioxidant compounds in *G. corneum*. Another study using *G. corneum* collected from the French Basque Coast also showed that different extraction conditions, including different solvent mixture, temperature and extraction time, impact the antioxidant potential (Castejón et al. 2021, 2024). Despite the varying methodologies used for extracting antioxidant candidates and assessing antioxidant activity, as well as the variability in the presentation of results, this seaweed is regarded as a seaweed species with low antioxidant capacity, and even aqueous extracts of *G. corneum* produced low to no antioxidant activity (Matos et al. 2020; Cavaco et al. 2021). Therefore, our results, although consistent with the previously reported range for the $DPPH^{\bullet}$ assay in aqueous extracts of *G. corneum* collected from the Portuguese Coast (5.57 ± 0.62 % to 10.89 ± 1.46 % inhibition), surpass the values reported for the $ABTS^{\bullet+}$ assay (10.85 ± 1.25 % to 13.90 ± 1.54 % inhibition) (Cavaco et al. 2021), highlighting lipids from *G. corneum* can be a potential source of antioxidant compounds.

Antioxidants can control the generation and/or scavenge reactive oxygen species and free radicals, interrupting free radical-mediated chain reactions (Lourenço et al. 2019). This helps reduce oxidative stress as well as inflammation, which are underlying factors in the development of several non-communicable diseases, including cardiovascular diseases or diabetes, as well as skin diseases, such as psoriasis, atopic dermatitis or acne vulgaris, by significantly contributing to skin damage and accelerating skin ageing (Thiyagarasaiyar et al. 2020; Conde et al. 2021; Zaid et al. 2022). Therefore, antioxidants have the potential to counterbalance the increase in oxidative stress, restore cellular homeostasis, and prevent various pathologies (Chaudhary et al. 2023; Jomova et al. 2023). However, oxidative damage also affects food products exposed to air, heat and/or light, leading to product deterioration as well as to undesirable smells and tastes (Geng et al. 2023). In recent years, there has been increasing interest in using natural antioxidants as a suitable alternative to synthetic ones, particularly in industrial sectors such as food, but also in cosmetics and cosmeceuticals. In the food industry, antioxidants are used to enhance stability, extend shelf-life, preserve nutritional quality, and improve functional properties of food products, minimizing oxidative processes and reducing microbiological proliferation, addressing consumer demands for safer, healthier, and longer-lasting food products (Hoang et al. 2021; Petcu et al. 2023). In cosmetics, antioxidants can protect skin against UV-induced photodamage, preventing oxidative damage and reducing skin aging (Thiyagarasaiyar et al. 2020; Hoang et al. 2021; Zaid et al. 2022),

while can enhance the antioxidant mechanisms of the skin itself (Hoang et al. 2021). The growing interest and the shift towards natural antioxidants are driven not only from their biological potential but also by safety concerns and potential adverse health effects associated with synthetic antioxidants and preservatives, as well as environmental issues related to the occurrence and fate of these compounds (Lourenço et al. 2019; Hoang et al. 2021). Moreover, natural antioxidants offer economic benefits, as they can be extracted from common plant sources as well as more sustainable resources like algae, food and plant-derived wastes/by-products, and underutilized plant species (Lourenço et al. 2019). Therefore, these findings suggest that lipids from *G. corneum* and its residue have potential applications as active ingredients for limiting oxidative stress and as natural additives to replace synthetic antioxidants in different industrial applications.

Lipids from both *G. corneum* samples exhibited noticeable anti-inflammatory activity. A previous study reported that ethanolic extracts from *G. corneum* (1 mg mL^{-1}) rich in polyphenols inhibited COX-2 activity in 54 ± 6% (Matos et al. 2020), while in our study, lipids from *G. corneum* at 50 µg mL^{-1} inhibited COX-2 activity by approximately 70%, suggesting a potentially greater capacity of lipids to inhibit enzyme activity. To our knowledge, only a few studies evaluated the inhibition of COX-2 by red seaweed lipids (Lopes et al. 2020; Costa et al. 2021). Lipids from *P. palmata* and *P. dioica* inhibited COX-2 activity by 89.9 ± 0.9 % and 83.6 ± 8.1% at 500 µg mL^{-1} (Lopes et al. 2020), respectively, while lipids from *G. turuturu* inhibited COX-2 activity by 50% at 33 µg mL^{-1} (Costa et al. 2021). Overall, these findings are consistent with the results observed for *G. corneum*, whose lipids showed greater capacity to inhibit enzymatic activity, particularly at lower concentrations. In the lipid profile of *G. corneum* there are several lipid species previously reported with anti-inflammatory properties, namely MGDG 36:4 (MGDG 20:4_16:0), MGDG 36:5 (MGDG 20:5_16:0), MGDG 40:9 (MGDG 20:5_20:4), MGDG 40:10 (20:5/20:5), DGDG 36:4 (DGDG 20:4_16:0), DGDG 36:5 (DGDG 20:5_16:0), SQDG 36:5 (SQDG 20:5_16:0), and LPC 16:0, as reviewed in (Conde et al. 2022). Fewer species with reported bioactivity were found in the residue, namely MGDG 36:5 (MGDG 20:5_16:0), DGDG 36:4 (DGDG 20:4_16:0), DGDG 36:5 (DGDG 20:5_16:0), and LPC 16:0, which may be due to the lower GL content in *G. corneum* residue obtained after agar extraction. Moreover, this may contribute to the lower anti-inflammatory potential observed for residue. Interestingly, several of these bioactive lipid species contain FA 20:5 *n*−3 (EPA), which can compete with FA 20:4 *n*−6 as a substrate for the COX-2 enzyme thereby shifting enzyme activity towards the production of anti-inflammatory mediators while limiting the production of pro-inflammatory ones (Kumar et al. 2019; Conde et al. 2021). Therefore, the observed reduction in COX-2-derived prostaglandins production may also be attributed to the competitive interaction between FA 20:5 *n*−3 and FA 20:4 *n*−6, rather than just to the direct inhibition of COX-2 activity.

Inflammation is a biological response against harmful stimuli (Mukhopadhyay et al. 2023). This is a tightly regulated and balanced process between pro-inflammatory and anti-inflammatory mediators (Mukhopadhyay et al. 2023). However, disruption of this balance can lead to an excessive production of pro-inflammatory mediators, such as prostaglandins, through upregulation of COX-2 activity (Attiq et al. 2018; Ju et al. 2022). This can result in prolonged or chronic inflammation, which is linked to a range of inflammatory-mediated diseases such as cardiovascular, neurodegenerative, autoimmune diseases, among others as well as skin diseases, where prostaglandins derived from COX-2 are responsible for acute inflammation of the skin (Ricciotti and Fitzgerald 2011; Conde et al. 2021). Therefore, managing and balancing inflammatory responses is essential to maintain health and prevent chronic conditions. COX-2 is an inducible enzyme triggered during inflammation, which catalyzes the conversion of arachidonic acid into pro-inflammatory prostaglandins and plays a key role in the inflammatory process (Attiq et al. 2018; Reis et al. 2020). Given its role, COX-2 has become a key target in searching for anti-inflammatory drugs to block prostaglandin biosynthesis (Reis et al. 2020). However, current COX-2 inhibitors are often associated with various adverse effects, prompting ongoing research into natural inhibitors with potent COX-2 inhibitory and anti-inflammatory properties (Attiq et al. 2018; Reis et al. 2020). Thus, these results suggest that lipids from *G. corneum* and its residue offer a novel natural and alternative source of compounds with potential as COX inhibitors.

Although the lipids from both *G. corneum* samples lacked α-amylase inhibitory activity, they were capable of inhibiting α-glucosidase. Despite the lack of data on the antidiabetic activity of bioactive compounds from *G. corneum*, acetone extracts of *Gelidium* sp. (but not ethanol extracts), containing polyphenols, inhibited α-amylase activity to 77.9 ± 2.1% at a concentration of 2000 µg of dry extract mL^{-1}. However, none of the extracts were able to inhibit α-glucosidase activity within the concentration range assessed (1, 10, 100, 1000 µg dry extract mL^{-1}) (Pacheco et al. 2020). Methanolic extracts of *G. amansii* inhibited α-glucosidase activity in 96.47% at 1 mg mL^{-1} (Ko et al. 2011).

The α-amylase and α-glucosidase are key enzymes in carbohydrate digestion, catalyzing the hydrolysis of starch into glucose within the intestine (Dirir et al. 2022; Şöhretoğlu et al. 2023). These enzymes significantly reduce postprandial blood glucose, making them important targets of antidiabetic drugs for managing blood glucose levels and controlling hyperglycemia (Dirir et al. 2022). Among the many diabetes-associated complications, skin problems are

highly prevalent, including diabetic dermopathy, dry skin, redness, and scarring (De Macedo et al. 2016; Azizian et al. 2019). Although inhibitors like acarbose can delay glucose absorption, they are often associated with undesirable gastrointestinal side effects (DiNicolantonio et al. 2015). As a result, ongoing research is focused on discovering novel, natural inhibitors that offer improved efficacy with fewer side effects. Hence, lipids from *G. corneum* and its residue can be explored as a promising source of novel bioactive compounds for non-pharmacological interventions aimed at improving glycemic control in the management of type 2 diabetes as well as in other related health conditions.

Conclusions

This lipidomics study revealed that *G. corneum* and its residue obtained after agar extraction contained a plethora of lipids, including essential FA and complex lipids with significant nutritional and functional value. The lipid pool of *G. corneum* was predominantly composed of GL, pigments, and phenolics, while the residue lipid pool was richer in PL and TG. Both samples included complex lipid species with the essential FA esterified, underscoring their nutritional quality. The identification of specific lipid classes as GL, commonly associated with anti-inflammatory properties, which was also corroborated by the inhibition of COX-2, and the demonstrated antioxidant and antiglycemic properties highlight the potential of *G. corneum* as novel food and as an alternative source of high-quality lipids. Additionally, *G. corneum* residue can be used to obtain lipid ingredients suitable for the food, nutraceutical, and cosmetics industries, with the higher content of Cer offering the potential to foster innovation in cosmetic products. Furthermore, *G. corneum* residue can be reused as a low-cost source of value-added lipids, contributing to a sustainable and circular blue bioeconomy perspective. Future studies should focus on exploring lipid extraction from *G. corneum* and its residue using biosolvents compatible with the food and cosmetic industries, such as ethanol. This approach may also enhance the recovery of bioactive lipids, such as GL and pigments, as well as other valuable compounds like phenolic compounds.

Supplementary Information The online version contains supplementary material available at https://doi.org/10.1007/s10811-025-03641-7.

Acknowledgments The authors are thankful to the project "Pacto da Bioeconomia azul" (Project No. C644915664-00000026) within the WP5 Algae Vertical, funded by Next Generation EU European Fund and the Portuguese Recovery and Resilience Plan (PRR), under the scope of the incentive line "Agendas for Business Innovation" through the funding scheme C5 - Capitalization and Business Innovation. This work is also funded by national funds through FCT – Fundação para a Ciência e a Tecnologia I.P., under the project/grant UID/50006 + LA/P/0094/2020 (https://doi.org/10.54499/LA/P/0094/2020; Centro de Estudos do Ambiente e Mar (CESAM)) and UID/50006 - Laboratório Associado para a Química Verde - Tecnologias e Processos Limpos. The authors also acknowledge to the University of Aveiro and to the Portuguese Mass Spectrometry Network – RNEM (LISBOA-01-0145-FEDER-402-022125). Thanks to Molecular Discovery Ltd for the Lipostar version 2.1.5 license. Joana Batista is grateful to FCT for her PhD Grant (2024.04123.BDANA). Tânia Melo thanks to FCT/MCTES for individual funding in the scope of the Individual Call to Scientific Employment Stimulus [CEECIND/01578/2020, https://doi.org/10.54499/2020.01578.CEECIND/CP1589/CT0010]. Rita Pais thanks for her PhD grant within the project "Pacto da Bioeconomia azul" (Project No. C644915664-00000026). Marisa Pinho was funded by national funds through the FCT-Foundation for Science and Technology, I.P., under the PhD granted via CESAM (UI/BD/153346/2022). Bruna B. Neves is grateful to FCT for her PhD Grant (https://doi.org/10.54499/2021.04602.BD).

Author contributions J.B. - Conceptualization, Investigation, Writing - review & editing, Writing - original draft, Formal analysis, Visualization; D.L., B. B. N., and A. R. P. - Investigation, Writing - review & editing; M. P., A. S. P. M, T. C., and P. D. - Methodology, Writing - review & editing; S. B. and L. G. - Methodology, Software, Writing - review & editing; J. D. and A. A. - Resources, Writing - review & editing; H. P. - Supervision, Resources, Writing - review & editing; M. R. D. - Conceptualization, Validation, Visualization, Writing - original draft, Writing - review & editing, Resources, Supervision; T. M. - Conceptualization, Methodology, Visualization, Validation, Writing - original draft, Writing - review & editing, Supervision. All authors reviewed the manuscript.

Funding This study was supported by the "Pacto da Bioeconomia azul" (Project No. C644915664-00000026) within the WP5 Algae Vertical, funded by Next Generation EU European Fund and the Portuguese Recovery and Resilience Plan (PRR), under the scope of the incentive line "Agendas for Business Innovation" through the funding scheme C5 - Capitalization and Business Innovation. This work is also funded by national funds through FCT – Fundação para a Ciência e a Tecnologia I.P., under the project/grant UID/50006 + LA/P/0094/2020 (https://doi.org/10.54499/LA/P/0094/2020; Centro de Estudos do Ambiente e Mar (CESAM)) and UID/50006 - Laboratório Associado para a Química Verde - Tecnologias e Processos Limpos.

Data availability The raw data are available from the corresponding author on reasonable request.

Declarations

Competing interests The authors declare no competing interests.

References

The Lipid Web (2023) The LipidWeb. https://www.lipidmaps.org/resources/lipidweb/index.php?page=ms/methesters/me-arch/index.htm. Accessed 20 Feb 2025

FIP (2025) Food and Feed Information Portal Database | FIP. https://ec.europa.eu/food/food-feed-portal/screen/novel-food-catalogue/search. Accessed 20 Feb 2025

Anon (2025b) COX-2 (human) Inhibitor Screening Assay Kit (Cyclooxygenase 2, PGHS-2, Prostaglandin H Synthase 2) | Cayman Chemical. https://www.caymanchem.com/product/701080/cox-2-(human)-inhibitor-screening-assay-kit. Accessed 20 Feb 2025

Abedi F, Hayes AW, Reiter R, Karimi G (2020) Acute lung injury: the therapeutic role of Rho kinase inhibitors. Pharmacol Res 155:104736

Ahmad A, Ahsan H (2020) Lipid-based formulations in cosmeceuticals and biopharmaceuticals. Biomed Dermatol 4:12

Ahmad S, Singh A, Akram W, Upadhyay A, Abrol GS (2025) Algal lipids: a review on current status and future prospects in food processing. J Food Sci 90:e17618

Alhajj MJ, Montero N, Yarce CJ, Salamanca CH (2020) Lecithins from vegetable, land, and marine animal sources and their potential applications for cosmetic, food, and pharmaceutical sectors. Cosmet 7:87

Álvarez-Viñas M, Flórez-Fernández N, Torres MD, Domínguez H (2019) Successful approaches for a red seaweed biorefinery. Mar Drugs 17:620

Atef B, Ishak RAH, Badawy SS, Osman R (2022) Exploring the potential of oleic acid in nanotechnology-mediated dermal drug delivery: an up-to-date review. J Drug Deliv Sci Technol 67:103032

Attiq A, Jalil J, Husain K, Ahmad W (2018) Raging the war against inflammation with natural products. Front Pharmacol 9:796

Avallone R, Vitale G, Bertolotti M (2019) Omega-3 fatty acids and neurodegenerative diseases: new evidence in clinical trials. Int J Mol Sci 20:4256

Azizian Z, Behrangi E, Hasheminasabzavareh R, Kazemlo H, Esmaeeli R, Hassani P (2019) Prevalence study of dermatologic manifestations among diabetic patients. Adv Prev Med 2019:5293193

Badimon L, Padró T, Vilahur G (2012) Atherosclerosis, platelets and thrombosis in acute ischaemic heart disease. Eur Heart J Acute Cardiovasc Care 1:60–74

Bell BM, Daniels DGH, Fearn T, Stewart BA (1987) Lipid compositions, baking qualities and other characteristics of wheat varieties grown in the U.K. J Cereal Sci 5:277–286

Berglund J, Azhar S, Lawoko M, Lindström M, Vilaplana F, Wohlert J, Henriksson G (2019) The structure of galactoglucomannan impacts the degradation under alkaline conditions. Cellulose 26:2155–2175

Castejón N, Parailloux M, Izdebska A, Lobinski R, Fernandes SCM (2021) Valorization of the red algae *Gelidium sesquipedale* by extracting a broad spectrum of minor compounds using green approaches. Mar Drugs 19:574

Castejón N, Adrien A, Spitzer L, Fernandes SCM (2024) Unlocking the full potential of the red seaweed *Gelidium corneum*: beyond its use as an agar source. J Appl Phycol 36:291–311

Cavaco M, Duarte A, Freitas MV, Afonso C, Bernardino S, Pereira L, Martins M, Mouga T (2021) Seasonal nutritional profile of *Gelidium corneum* (Rhodophyta, Gelidiaceae) from the center of Portugal. Foods 10:2394

Chan PT, Matanjun P (2017) Chemical composition and physicochemical properties of tropical red seaweed, *Gracilaria changii*. Food Chem 221:302–310

Chaudhary P, Janmeda P, Docea AO, Yeskaliyeva B, Razis AFBR, Modu B, Calina D, Sharifi-Rad J (2023) Oxidative stress, free radicals and antioxidants: potential crosstalk in the pathophysiology of human diseases. Front Chem 11:1158198

Chen J, Liu H (2020) Nutritional indices for assessing fatty acids: a mini-review. Int J Mol Sci 21:5695

Conde T, Lopes D, Łuczaj W, Neves B, Pinto B, Maurício T, Domingues P, Skrzydlewska E, Domingues MR (2022) Algal lipids as modulators of skin disease: a critical review. Metabolites 12:96

Conde T, Lopes D, Pinho M, Melo T, Coelho N, Rodrigues AMC, Pereira H, Domingues P, Domingues R (2025) Unraveling the lipidome of *Pavlova gyrans*, a natural reservoir of bioactive lipids for biotechnological applications. J Appl Phycol 37:855–871

Conde T, Neves B, Couto D, Melo T, Lopes D, Rita Pais, Batista J, Cardoso H, Silva JL, Domingues P, Domingues MR (2023) Polar lipids of marine microalgae *Nannochloropsis oceanica* and *Chlorococcum amblystomatis* mitigate the LPS-induced pro-inflammatory response in macrophages. Mar Drugs 21:629

Conde T, Zabetakis I, Tsoupras A, Medina I, Costa M, Silva J, Neves B, Domingues P, Domingues MR (2021) Microalgal lipid extracts have potential to modulate the inflammatory response: a critical review. Int J Mol Sci 22:9825

Costa E, Melo T, Reis M, Domnigues P, Calado R, Abreu MH, Domingues MR (2021) Polar lipids composition, antioxidant and anti-inflammatory activities of the Atlantic red seaweed *Grateloupia turuturu*. Mar Drugs 19:414

Couto D, Melo T, Conde TA, Costa M, Silva J, Domingues MRM, Domingues P (2021) Chemoplasticity of the polar lipid profile of the microalgae *Chlorella vulgaris* grown under heterotrophic and autotrophic conditions. Algal Res 53:102128

da Costa E, Azevedo V, Melo T, Rego AM, Evtuguin DV, Domingues P, Calado R, Pereira R, Abreu MG, Domingues MR (2018) High-resolution lipidomics of the early life stages of the red seaweed *Porphyra dioica*. Molecules 23:187

Da Costa E, Melo T, Moreira ASP, Bernardo C, Helguero L, Ferreira I, Cruz MT, Rego AM, Domingues P, Calado R, Abreu MH, Domingues MR (2017) Valorization of lipids from *Gracilaria sp.* through lipidomics and decoding of antiproliferative and anti-inflammatory activity. Mar Drugs 15:62

De Luca M, Pappalardo I, Limongi AR, Viviano E, Radice RP, Todisco S, Martelli G, Infatino V, Vassalo A (2021) Lipids from microalgae for cosmetic applications. Cosmet 8:52

De Macedo GMC, Nunes S, Barreto T (2016) Skin disorders in diabetes mellitus: an epidemiology and physiopathology review. Diabetol Metab Syndr 8:63

DiNicolantonio JJ, Bhutani J, O'Keefe JH (2015) Acarbose: safe and effective for lowering postprandial hyperglycaemia and improving cardiovascular outcomes. Open Hear 2:e000327

Dirir AM, Daou M, Yousef AF, Yousef LF (2022) A review of alpha-glucosidase inhibitors from plants as potential candidates for the treatment of type-2 diabetes. Phytochem Rev 21:1049–1079

Djuricic I, Calder PC (2023) Pros and cons of long-chain omega-3 polyunsaturated fatty acids in cardiovascular health. Annu Rev Pharmacol Toxicol 63:383–406

Dongho Dongmo FF, Fogang Mba AR, Njike Ngamga FH, Asongni WD, Zokou R, Noutsa BS, Hagbe DN, Tchuenbou-Magaia FL, Ebelle Etame RM (2024) An overview of fatty acids-based nutritional quality indices of fish oils from Cameroon: impact of fish pre-treatment and preservation methods. J Food Compos Anal 131:106250

Errati H, Bencheqroun SK, Aboutayeb R, Abail Z, Lebbar S, Dari K, Hilali L (2022) Assessment of the red seaweed *Gelidium sesquipedale* by-products as an organic fertilizer and soil amendment. Sustainability 14:14217

Ferreira M, Salgado JM, Peres H, Belo I (2024) Valorization of *Gelidium corneum* by-product through solid-state fermentation. Food Bioprod Process 146:205–212

Ferrera-Lorenzo N, Fuente E, Suárez-Ruiz I, Gil RR, Ruiz B (2014) Pyrolysis characteristics of a macroalgae solid waste generated by the industrial production of agar-agar. J Anal Appl Pyrolysis 105:209–216

Freitas MV, Inácio LG, Martins M, Afonso C, Pereira L, Mouga T (2022) Primary composition and pigments of 11 red seaweed species from the center of Portugal. J Mar Sci Eng 10:1168

Geng L, Liu K, Zhang H (2023) Lipid oxidation in foods and its implications on proteins. Front Nutr 10:1192199

Gomes-Dias JS, Romaní A, Teixeira JA, Rocha CMR (2020) Valorization of seaweed carbohydrates: autohydrolysis as a selective and sustainable pretreatment. ACS Sustain Chem Eng 8:17143–17153

Gomes-Dias JS, Teixeira-Guedes CI, Teixeira JA, Rocha CMR (2024) Red seaweed biorefinery: the influence of sequential extractions on the functional properties of extracted agars and porphyrans. Int J Biol Macromol 257:128479

Gonzalez-Becerra K, Barron-Cabrera E, Muñoz-Valle JF, Torres-Castillo N, Rivera-Valdes JJ, Rodriguez-Echevarria R, Martinez-Lopez E (2023) A balanced dietary ratio of n-6:n-3 polyunsaturated fatty acids exerts an effect on total fatty acid profile in RBCs and inflammatory markers in subjects with obesity. Healthcare 11:2333

Goracci L, Tortorella S, Tiberi P, Pellegrino RM, Di Veroli A, Valeri A, Cruciani G (2017) Lipostar, a comprehensive platform-neutral cheminformatics tool for lipidomics. Anal Chem 89:6257–6264

Grina F, Ullah Z, Kaplaner E, Moujahid A, Eddoha R, Nasser B, Terzioğlu P, Abdullah Yilmaz M, Ertaş A, Öztürk M, Essamadi A (2020) In vitro enzyme inhibitory properties, antioxidant activities, and phytochemical fingerprints of five Moroccan seaweeds. S Afr J Bot 128:152–160

Harrysson H, Krook JL, Larsson K, Tullberg C, Oerbekke A, Toth G, Pavia H, Undeland I (2021) Effect of storage conditions on lipid oxidation, nutrient loss and colour of dried seaweeds, *Porphyra umbilicalis* and *Ulva fenestrata*, subjected to different pretreatments. Algal Res 56:102295

Hinder A, Schmelzer CEH, Rawlings AV, Neubert RHH (2011) Investigation of the molecular structure of the human stratum corneum ceramides [NP] and [EOS] by mass spectrometry. Skin Pharmacol Physiol 24:127–135

Hoang HT, Moon JY, Lee YC (2021) Natural antioxidants from plant extracts in skincare cosmetics: Recent applications, challenges and perspectives. Cosmetics 8:106

Jomova K, Raptova R, Alomar SY, Alwasel SH, Nepovimova E, Kuca K, Valko M (2023) Reactive oxygen species, toxicity, oxidative stress, and antioxidants: chronic diseases and aging. Arch Toxicol 97:2499–2574

Ju Z, Li M, Xu J, Howell DC, Li Z, Chen FE (2022) Recent development on COX-2 inhibitors as promising anti-inflammatory agents: the past 10 years. Acta Pharm Sin B 12:2790–2807

Kawana M, Miyamoto M, Ohno Y, Kihara A (2020) Comparative profiling and comprehensive quantification of stratum corneum ceramides in humans and mice by LC/MS/MS. J Lipid Res 61:884–895

Kawashima H (2019) Intake of arachidonic acid-containing lipids in adult humans: dietary surveys and clinical trials. Lipids Health Dis 18:101

Kim OY, Song J (2024) Important roles of linoleic acid and α-linolenic acid in regulating cognitive impairment and neuropsychiatric issues in metabolic-related dementia. Life Sci 337:122356

Knox S, Boyle NMO (2021) Skin lipids in health and disease: a review. Chem Phys Lipids 236:105055

Ko SC, Lee SH, Kang SM, Ahn G, SH Cha, Jeon SH (2011) Evaluation of α-glucosidase inhibitory activity of jeju seaweeds using high throughput screening (HTS) technique. J Mar Biosci Biotechnol 5:33–39

Kumar M, Kumari P, Trivedi N, Shukla MK, Gupta V, Reddy CRK, Jha B (2011) Minerals, PUFAs and antioxidant properties of some tropical seaweeds from Saurashtra coast of India. J Appl Phycol 23:797–810

Kumar N, Contaifer D, Madurantakam P, Carbone S, Price ET, Tassel BV, Brophy DF, Wijesinghe DS (2019) Dietary bioactive fatty acids as modulators of immune function: implications on human health. Nutrients 11:2974

Lebbar S, Fanuel M, Le Gall S, Falourd X, Ropartaz D, Bressollier P, Gloaguen V, Faugeron-Girard C (2018) Agar extraction by-products from *Gelidium sesquipedale* as a source of glycerol-galactosides. Molecules 23:3364

Li Y, Ghasemi Naghdi F, Garg S, Adarme-Vega TC, Thurecht KJ, Ghafor WA, Tannock Schenk PM (2014) A comparative study: the impact of different lipid extraction methods on current microalgal lipid research. Microb Cell Fact 13:14

Li Y, He N, Hou J, Liu C, Zhang J, Wang Q, Zhang X, Wu X (2018) Factors influencing leaf chlorophyll content in natural forests at the biome scale. Front Ecol Evol 6:00064

Libbey LM, Walradt JP (1968) Analysis of total phenols and other oxidation substrates and antioxidants by means of Folin-Ciocalteu reagent. Meth Enzymol 3:561

Liebisch G, Fahy E, Aoki J, Dennis EA, Durand T, Ejsing CS, Fedorova M, Feussner I, Griffins WJ, Köfeler H, Merrill AH Jr, Murphy RC, O'Donnell VB, Oskolkova O, Subramaniam Wakelam MJO, Spener F (2020) Update on LIPID MAPS classification, nomenclature, and shorthand notation for MS-derived lipid structures. J Lipid Res 61:1539–1555

Liu Y, Shen N, Xin H, Yu Lili, Xu Qinq, Cui Yulei (2023) Unsaturated fatty acids in natural edible resources, a systematic review of classification, resources, biosynthesis, biological activities and application. Food Biosci 53:102790

Lopes D, Melo T, Meneses J, Abreu MH, Pereira R, Domingues P, Lillebø AI, Calado R, Domingues MR (2019) A new look for the red macroalga *Palmaria palmata*: a seafood with polar lipids rich in EPA and with antioxidant properties. Mar Drugs 17:533

Lopes D, Melo T, Rey F, Meneses J, Monteiro FL, Helguero LA, Abreu MH, Lillebø AI, Calado R, Domingues MR (2020) Valuing bioactive lipids from green, red and brown macroalgae from aquaculture, to foster functionality and biotechnological applications. Molecules 25:3883

Lopes D, Moreira ASP, Rey F, da Costa E, Melo T, Maciel E, Rego A, Abreu MH, Domingues P, Calado R, Lillebø AI, Domingues MR (2019) Lipidomic signature of the green macroalgae *Ulva rigida* farmed in a sustainable integrated multi-trophic aquaculture. J Appl Phycol 31:1369–1381

López-Hortas L, Flórez-Fernández N, Torres MD, Ferreira-Anta T, Casas MP, Balboa EM, Falqué E, Domínguez H (2021) Applying seaweed compounds in cosmetics, cosmeceuticals. Mar Drugs 19:552

Lourenço SC, Moldão-Martins M, Alves VD (2019) Antioxidants of natural plant origins: from sources to food industry applications. Molecules 24:4132

Lu W, Shi Y, Wang R, Su Deding, Tang M, Liu Y, Li Z (2021) Antioxidant activity and healthy benefits of natural pigments in fruits: a review. Int J Mol Sci 22:4945

Lu Y, Zhao J, Xin Q, Yuan R, Miao Y, Yang M, Mo H, Chen K, Cong W (2024) Protective effects of oleic acid and polyphenols in extra virgin olive oil on cardiovascular diseases. Food Sci Hum Wellness 13:529–540

Mank V, Polonska T (2016) Use of natural oils as bioactive ingredients of cosmetic products. Ukr Food J 5:281–289

Marangoni F, Agostoni C, Borghi C, Catapeno AL, Cena H, Ghiselli A, Vecchia La, Lercker G, Manzato E, Pirillo A, Riccardi G, Risé P, Visioli F, Poli A (2020) Dietary linoleic acid and human health: focus on cardiovascular and cardiometabolic effects. Atherosclerosis 292:90–98

Martínez-Sanz M, Gomez-Barrio LP, Zhao M, Tiwari B, Knutsen SV, Balance S, Zobel HK, Nilsson AE, Krewer C, Östergren K, López-Rubio A (2021) Alternative protocols for the production of more sustainable agar-based extracts from *Gelidium sesquipedale*. Algal Res 55:102254

Martínez-Sanz M, Cebrián-Lloret V, Mazarro-Ruiz J, López-Rubio A (2020) Improved performance of less purified cellulosic films obtained from agar waste biomass. Carbohydr Polym 233:115887

Martínez-Sanz M, Gómez-Mascaraque LG, Ballester AR, Martínez-Abad A, Brodkorb A, López-Rubio A (2019) Production of unpurified agar-based extracts from red seaweed *Gelidium sesquipedale* by means of simplified extraction protocols. Algal Res 38:101420

Mateus M, Mão de Ferro R, Pinheiro HM, Machado R, da Fonseca MMR, Sapatinha M, Pires C, Marmelo I, Marques A, Nunes ML, Motta C, Ceário MT (2024) Production and characterization of protein-rich extracts from the red macroalga *Gelidium corneum* and its industrial agar extraction residues. Algal Res 78:103420

Matias M, Martins A, Alves C, Silva J, Pinteus S, Fitas M, Pinto P, Marto J, Ribeiro H, Murray P, Pedrosa R (2023) New insights into the dermocosmetic potential of the red seaweed *Gelidium corneum*. Antioxidants 12:1684

Matos J, Gomes A, Cardoso C, Afonso C, Campos AM, Gomes R, Falé P, Delgado I, Coelho I, Castanheira I, Bandarra NM (2020) Commercial red seaweed in Portugal (*Gelidium sesquipedale* and *Pterocladiella capillacea*, Florideophyceae): going beyond a single-purpose product approach by valorizing bioactivity. Thalassas 36:213–224

McCusker MM, Grant-Kels JM (2010) Healing fats of the skin: the structural and immunologic roles of the Ω-6 and Ω-3 fatty acids. Clin Dermatol 28:440–451

Meinita MDN, Harwanto D, Amron Hannan MA, Jeong G-T, Moon IS, Choi J-S (2023) A concise review of the potential utilization based on bioactivity and pharmacological properties of the genus *Gelidium* (Gelidiales, Rhodophyta). J Appl Phycol 35:1499–1523

Melo T, Alves E, Azevedo V, Martins AS, Neves B, Domingues P, Calado R, Abreu MH, Domingues MR (2015) Lipidomics as a new approach for the bioprospecting of marine macroalgae — unraveling the polar lipid and fatty acid composition of *Chondrus crispus*. Algal Res 8:181–191

Melo T, Marques SS, Ferreira I, Cruz MT, Domingues P, Segundo MA, Domingues MRM (2018) New insights into the anti-inflammatory and antioxidant properties of nitrated phospholipids. Lipids 53:117–131

Monteiro JP, Sousa T, Pinho M, Moreira A, Goracci L, Pires C, Marques A, Nunes ML, Domingues P, Calado R, Domingues MR (2025) Comparative lipid analysis and valorization strategies for processed gilthead seabream and European pilchard secondary raw materials. LWT 225:117888

Moreira ASP, da Costa E, Melo T, Lopes D, Pais ACS, Santos SÃO, Pitarma B, Mendes M, Abreu MG, Collén PN, Domingues P, Domingues MR (2021) Polar lipids of commercial *Ulva spp*. of different origins: Profiling and relevance for seaweed valorization. Foods 10:914

Mouga T, Fernandes IB (2022) The red seaweed giant *Gelidium* (*Gelidium corneum*) for new bio-based materials in a circular economy framework. Earth 3:788–813

Mukhopadhyay N, Shukla A, Makhal PN, Kaki VR (2023) Natural product-driven dual COX-LOX inhibitors: overview of recent studies on the development of novel anti-inflammatory agents. Heliyon 9:e14569

Munteanu IG, Apetrei C (2021) Analytical methods used in determining antioxidant activity: a review. Int J Mol Sci 22:3380

Nassar M, Jaffery A, Ibrahim B, Baraka B, Aboshaeaishaa H (2023) The multidimensional benefits of eicosapentaenoic acid: from heart health to inflammatory control. Egypt J Intern Med 35:81

Navarro López E, Jiménez Callejón MJ, Macías Sánchez MD, González Moreno PA, Robles Medina A (2023) Obtaining eicosapentaenoic acid-enriched polar lipids from microalga *Nannochloropsis sp.* by lipase-catalysed hydrolysis. Algal Res 71:103073

Neves BB, Pinto S, Pais AR, Batista J, Pinho M, Goracci L, Domingues P, Domingues MR, Melo T (2025) Avocado by-products: recycling low-cost lipids towards high-end applications. LWT 216:117376

Oppedisano F, Macrì R, Gliozzi M, Musolino V, Carresi C, Maiuolo J, Bosco F, Nucera S, Zito MC, Guarnieri L, Scarano F, Nicita C, Coppoletta AR, Ruga S, Scicchitano M, Mollace R, Palma E, Mollace V (2020) The anti-inflammatory and antioxidant properties of n-3 PUFAs: their role in cardiovascular protection. Biomedicines 8:306

Pacheco LV, Parada J, Pérez-Correa JR, Mariotti-Celis MS, Erpel F, Zambrano A, Palacios M (2020) Bioactive polyphenols from southern Chile seaweed as inhibitors of enzymes for starch digestion. Mar Drugs 18:353

Pais R, Conde T, Neves BB, Pinho M, Coelho M, Pereira H, Rodrigues AMC, Domingues P, Gomes AM, Urbatzka R, Domingues R, Melo T (2024) Bioactive lipids in *Dunaliella salina*: implications for functional foods and health. Foods 13:3321

Paiva L, Lima E, Neto AI, Marcone M, Baptista J (2016) Health-promoting ingredients from four selected Azorean macroalgae. Food Res Int 89:432–438

Pereira TF, Borchardt H, Wanderley WF, asconcelos U, Leite IF (2025) Pequi pulp (*Caryocar brasiliense*) oil-loaded emulsions as cosmetic products for topical use. Polymers 17:226

Pereira SG, Teixeira-Guedes C, Souza-Matos G, Maricato E, Nunes C, Coimbra MA, Teixeira JA, Pereira RN, Rocha CMR (2021) Influence of ohmic heating in the composition of extracts from *Gracilaria vermiculophylla*. Algal Res 58:102360

Petcu CD, Tăpăloagă D, Mihai OD, Gheorghe-Irimia RA, Negoiță C, Georgescu IM, Tăpăloagă PR, Borda C, Ghimpețeanu OM (2023) Harnessing natural antioxidants for enhancing food shelf life: exploring sources and applications in the food industry. Foods 12:3176

Reis C, Barreto M, de Faria Menezes, Pereira S, da Cruz LL, de Sousa Passos M, de Moraes LP, Vieira IJC, de Oliveira DB (2020) Plants as sources of anti-inflammatory agents. Molecules 25:3726

Rey F, Cartaxana P, Melo T, Calado R, Pereira R, Abreu H, Domingues P, Cruz S, Domingues MR (2020) Domesticated populations of *Codium tomentosum* display lipid extracts with lower seasonal shifts than conspecifics from the wild — relevance for biotechnological applications of this green seaweed. Mar Drugs 18:188

Ricciotti E, Fitzgerald GA (2011) Prostaglandins and inflammation. Arterioscler Thromb Vasc Biol 31:986–1000

Risé P, Tragni E, Ghezzi S, Agostini C, Marangoni F, Poli A, Catapano AL, Siani A, Iacoviello L, Galli C (2013) Different patterns characterize omega 6 and omega 3 long chain polyunsaturated fatty acid levels in blood from Italian infants, children, adults and elderly. Prostaglandins Leukot Essent Fatty Acids 89:215–220

Safafar H, Wagenen J Van, Møller P, Jacobsen C (2015) Carotenoids, phenolic compounds and tocopherols contribute to the antioxidative properties of some microalgae species grown on industrial wastewater. Mar Drugs 13:7339–7356

Santos R, Melo RA (2018) Global shortage of technical agars: back to basics (resource management). J Appl Phycol 30:2463–2473

Şöhretoğlu D, Renda G, Arroo R, Xiao J, Sari S (2023) Advances in the natural α-glucosidase inhibitors. eFood 4:e112

Song Y, Wang H, Wang X, Wang X, Cong P, Xu J, Xue C (2023) Comparative lipidomics study of four edible red seaweeds based on RPLC-Q-TOF. J Agric Food Chem 71:2183–2196

Spector AA, Kim HY (2015) Discovery of essential fatty acids. J Lipid Res 56:11–21

Susanto E, Fahmi AS, Hosokawa M, Miyashita K (2019) Variation in lipid components from 15 species of tropical and temperate seaweeds. Mar Drugs 17:630

Taouam I, El Bouqdaoui K, Ridaoui K, Bourjilat F, Kabine M, Maata N, Cherki M (2024) Nutritional profile, phytochemical composition, antioxidant and antibacterial activities of *Gelidium corneum* from Dar Bouazza, Morocco. Egypt J Aquat Res 50:516–527

Thiyagarasaiyar K, Goh B, Jeon Y (2020) Algae metabolites in cosmeceutical: an overview of current applications and challenges. Mar Drugs 18:323

Tilami SK, Kouřimská L (2022) Assessment of the nutritional quality of plant lipids using atherogenicity and thrombogenicity indices. Nutrients 14:3795

Timalsina D, Bhusal D, Devkota HP, Pokhrel KP, Sharma KR (2021) α-amylase inhibitory activity of *Catunaregam spinosa* (Thunb.) Tirveng.: in vitro and in silico studies. BioMed Res Int 2021:4133876

Trigueros E, Sanz MT, Alonso-Riaño P, Beltrán S, Ramos C, Melgosa R (2021) Recovery of the protein fraction with high antioxidant activity from red seaweed industrial solid residue after agar extraction by subcritical water treatment. J Appl Phycol 33:1181–1194

Trigueros E, Sanz MT, Filipigh A, Beltrãn S, Riaño (2021b) Enzymatic hydrolysis of the industrial solid residue of red seaweed after agar extraction: Extracts characterization and modelling. Food Bioprod Process 126:356–366

Tůma S, Izaguirre JK, Bondar M, Marques MM, Fernandes P, da Fonseca MMR (2020) Upgrading end-of-line residues of the red seaweed *Gelidium sesquipedale* to polyhydroxyalkanoates using *Halomonas boliviensis*. Biotechnol Rep 27:e00491

Vega J, Bonomi-Barufi J, Gómez-Pinchetti JL, Figueroa FL (2020) Cyanobacteria and red macroalgae as potential sources of antioxidants and UV radiation-absorbing compounds for cosmeceutical applications. Mar Drugs 18:659

Wang B, Wu L, Chen J, Dong L, Chen C, Wen Z, Hu J, Fleming I (2021) Wang DW (2021) Metabolism pathways of arachidonic acids: mechanisms and potential therapeutic targets. Signal Transduct Target Ther 6:94

Wang LJ, Fan Y, Parsons RL, Hu GR, Zhang PY, Li FL (2018) A rapid method for the determination of fucoxanthin in diatom. Mar Drugs 16:33

Wang X, Jia Y, He H (2025) The role of linoleic acid in skin and hair health: a review. Int J Mol Sci 26:246

Weinman EO, Chaikoff IL, Entenman C, Dauben WG (1950) Turnover rates of phosphate and fatty acid moietiesof plasma phospholipides. J Biol Chem 187:643–649

Yang Y, Xia Y, Zhang B, Li D, Yan J, Yang J, Sun J, Cao H, Wang Y, Zhang F (2023) Effects of different n-6/n-3 polyunsaturated fatty acids ratios on lipid metabolism in patients with hyperlipidemia: a randomized controlled clinical trial. Front Nutr 10:1166702

Zaid NAM, Sekar M, Bonam SR, Gan SH, Lum PT, Begum MY, Mat Rani NNI, Vaijanathappa J, Wu YS, Subramaniyan V, Fuloria NK, Fuloria S (2022) Promising natural products in new drug design, development, and therapy for skin disorders: an overview of scientific evidence and understanding their mechanism of action. Drug Des Devel Ther 16:23–66

Zhang Y, Liu Y, Sun J, Zhang W, Guo Z, Ma Q (2023) Arachidonic acid metabolism in health and disease. MedComm 4:e363